Journal Pre-proof

Stratigraphic revision of the El Imperial Formation (Pennsylvanian-Cisuralian), in its type locality, San Rafael Basin(Mendoza), Argentina

M.S. Vázquez, C.O. Limarino, S.N. Césari

PII: S0895-9811(19)30292-5

DOI: https://doi.org/10.1016/j.jsames.2019.102365

Reference: SAMES 102365

To appear in: *Journal of South American Earth Sciences*

Received Date: 15 June 2019

Revised Date: 18 September 2019

Accepted Date: 18 September 2019

Please cite this article as: Vázquez, M.S., Limarino, C.O., Césari, S.N., Stratigraphic revision of the El Imperial Formation (Pennsylvanian-Cisuralian), in its type locality, San Rafael Basin(Mendoza), Argentina, *Journal of South American Earth Sciences* (2019), doi: https://doi.org/10.1016/j.jsames.2019.102365.

This is a PDF file of an article that has undergone enhancements after acceptance, such as the addition of a cover page and metadata, and formatting for readability, but it is not yet the definitive version of record. This version will undergo additional copyediting, typesetting and review before it is published in its final form, but we are providing this version to give early visibility of the article. Please note that, during the production process, errors may be discovered which could affect the content, and all legal disclaimers that apply to the journal pertain.

© 2019 Published by Elsevier Ltd.

Journal Pre-proof

Stratigraphic revision of the El Imperial Formation (Pennsylvanian-Cisuralian), in its type locality, San Rafael Basin(Mendoza), Argentina.

Vázquez, M.S.[a], Limarino, C.O.[b, *] and Césari, S.N.[c]

[a] Grupo Vinculado al IANIGLA, CONICET, Museo de Historia Natural de San Rafael, Parque Mariano Moreno s/n, 5600 San Rafael, Mendoza, Argentina. mariasolevazquez@gmail.com

[b] IGEBA-CONICET, Departamento de Geología, Facultad de Ciencias Exactas y Naturales, Universidad de Buenos Aires, Intendente Güiraldes 2160, Pabellón 2, Ciudad Universitaria, 1° piso, C1428EHA, Buenos Aires, Argentina. oscarlimarino@gmail.com

[c] Museo Argentino de Cs. Naturales B. Rivadavia, CONICET, Av. Ángel Gallardo 470, C1405DJR Buenos Aires, Argentina. silviancesari@gmail.com

*Corresponding author

Journal Pre-proof

Highlights

. Type section of the El Imperial Formation is revised.
. Eight facies associations represent sedimentation in glacial to postglacial conditions.
. Palynological associations belong to the DM and FS Biozones.
. A continuous late Sepurkhovian-earliest Cisuralian interval is recorded.

Journal Pre-proof

ABSTRACT. The El Imperial Formation (San Rafael Basin) shows a complete record of the late Carboniferous - early Permian stratigraphy in western basins of Argentina. The sedimentological and stratigraphic analysis in the type locality allowed recognizing eight facies associations. Facies association A includes diamictites and conglomerates related to the Late Paleozoic glacial event, facies B composed of shales and fine-grained sandstones, was formed during the postglacial transgression while facies C represents sandy littoral bars, that pass upward to shales and mudstones of the facies association D. The conglomerates and sandstones of the facies association E entirely correspond to fluvial sedimentation, followed by a new transgressive event represented in fine-grained sandstones and shales of the facies F. The last transgression is recorded in shales, mudstones and very fine-grained sandstones belonging to the facies G, which are covered by sandstones and conglomerates corresponding to multi-channel fluvial systems. From these facies associations, 33 palynofloras divided into three palynological associations were obtained. The palynological assemblages that characterized the basal section contain abundant trilete spores and monosaccate pollen grains, with a progressive increase of taeniate pollen towards the top of the unit. The presence of scolecodonts characterizes palynofloras from transitional to marine environments. The composition of the palynofloras allows correlations with the current biostratigraphic scheme of the center-west of Argentina. The presence of the Biozone *Raistrickia densa- Convolutispora muriornata* in the lower and middle part of the El Imperial Formation, together with *Pakhapites fusus-Vittatina subsaccata* Biozone in the upper part, allows us to refer the palynofloras to the late Serpukhovian / early Cisuralian.

Keywords. Paleoenvironment**,** Palynology, Carboniferous, Permian, El Imperial Formation.

Journal Pre-proof

Journal Pre-proof

1. Introduction

The San Rafael Basin (Mendoza Province) offers one of the more complete stratigraphic records of the Late Paleozoic sedimentation in the western Gondwana, recording the transition from icehouse conditions (Late Mississippian), to postglacial (Pennsylvanian), and then environments subject to very intense volcanism and extreme greenhouse climates (Middle and Late Permian, Limarino et al., 2014a). Glacial and postglacial sedimentation corresponds to the El Imperial Formation (Dessanti, 1945, 1956), while volcanism and volcaniclastic sedimentation comprise to the Cochicó Group (Dessanti, 1956).

Dessanti (1945, 1956) made the first discovery of fossils at the north of the Diamante River, describing the fossiliferous strata as the Imperial System and later as the Imperial Series. This locality, known as Arroyo El Imperial (Fig. 1), is considered the type area of the unit and formally nominated as a lectostratotype by Pazos et al. (2017). Espejo (1990) and Espejo and López-Gamundí (1994), made sedimentological studies of the type locality (Arroyo El Imperial) and other equivalents outcrops in the surroundings of the Atuel Canyon. New results on the sedimentology of the formation were presented by Pazos et al. (2007, 2017) and Henry et al. (2014), at the Atuel Canyon area (Fig. 1).

The Late Paleozoic record of the San Rafael Basin was studied due to their excellent exposures and fossil content; however, the palynological information, known up to now (Azcuy and Gutiérrez, 1985, García and Azcuy, 1987, García, 1990, 1992, 1995, 1996, Pazos et al., 2007), results insufficient to make a precise correlation with other basins of Argentina.
In this paper, is analyzed the paleoenvironmental evolution of the El Imperial Formation in the type locality (Arroyo El Imperial), and nearby sections in the Atuel Canyon area (Rincón Bayo creek, Fig. 1) and the Camino del Baqueano (Los Reyunos dam, Fig. 1). A detailed palynological sampling made it possible to relate the palynofloras to the facies associations and thus characterize palynologically the continental, transitional and marine successions deposited in environments affected by glacial and postglacial conditions (Pazos, 2002, López-Gamundí,

Journal Pre-proof

2010).

Even though the first references to these Carboniferous rocks correspond to Stappenbeck (1934), who assigned them as strata of the "Paganzo Inferior", the knowledge about the relationship between palynological and paleoenvironmental evolution of the El Imperial Formation in the type locality is yet incomplete since the major part of the studies were made away from the type locality. In order to the knowledge of the Carboniferous succession be improved, a stratigraphic revision of the El Imperial Formation in its type locality is presented.

2. Previous studies

Dessanti (1945) and later Giudici (1971) made the first studies in the area and recognized two members in the El Imperial Formation; the Lower Member is composed of sandstones, shales, siltstones, and conglomerates, while the Upper Member is made up by sandstones and conglomerates.

Arias and Azcuy (1986) described another stratigraphic section in the Atuel Canyon, close to the Aisol creek (Fig. 1). The mentioned authors recognized four sedimentary facies and three depositional episodes, two marines to transitional (infill of submarine valleys and deltaic body) and one continental (channels and bars of anastomosed rivers).

Later, Espejo (1990), and Espejo et al. (1996) described three main depositional episodes in the El Imperial Formation, between Represa Agua del Toro and Atuel Canyon. The first stage corresponds to an initial transgressive fill dominated by glacimarine sedimentation represented in diamictites and shales bearing dropstones. The second stage represents fluvial-deltaic sedimentation, including low-sinuosity river, lacustrine, deltaic and shallow marine environments. Finally, in the third stage, a definitive continentalization (low-sinuosity river deposits) and reversal of the regional slope were recognized (Espejo et al., 1996). Pazos et al. (2007) described for the Arroyo Aisol, in the Atuel Canyon, a lower unit characterized by shallow water deposits in a paleovalley linked to a glacial area and a middle unit that represents a fjord

Journal Pre-proof

environment.

Espejo and Lopez Gamundí (1994) divided the El Imperial Formation in four facies associations and studied the sandstone composition of the deltaic deposits, including wave-reworked channel mouth-bar and fluvial-dominated distributary channel facies.

In recent years, Henry et al. (2014) analyzed in detail the lower and middle sections of the El Imperial Formation at the Atuel Canyon area, describing shallow marine glacial influenced deposits that pass upward into postglacial open marine sequences.

Recently, Pazos et al. (2017), proposed the Arroyo Aisol (Atuel Canyon) section as a hypostratotype for the El Imperial Formation. The authors defined and described in detail two members: Glacial and Cabecera del Cañón Members, which represent glacial influenced sedimentation in paleofjord environments and open marine deposits, respectively.

3. Description of the type section

The geology of the area is shown in Figure 2, the local basement corresponds to metasedimentary rocks included in the La Horqueta Formation composed of slates, sandstones and shales intruded by abundant dikes and veins of quartz. These rocks crop out in the north and west of the studied area, forming from metric- to decametric-scale folds and intricate patterns of faults.

The contact between La Horqueta beds and the overlying El Imperial Formation (860 m thick) is tectonic in the north of the area, and normal in the west (Fig. 2), where the surface is highly irregular, suggesting the development of a sharp paleo-relief before the deposition of the El Imperial Formation.

The El Imperial Formation crops out forming a south-west dipping homoclinal succession, affected by minor strike-faults of some tens of meters of displacement and small scale folds (Fig. 2). The Permian volcaniclastic succession belonging to the Cochicó Group overlies the El Imperial Formation in the west of the studied region through an erosive unconformity (Fig.

Journal Pre-proof

2).

Detailed sedimentary sections were obtained that allowed to recognize eight facies associations (Figs. 3 and 4, Table 1). Each facies association was sampled for palynological analysis, which allowed obtaining a complete palynostratigraphic record of the unit in the type area.

Additional information was obtained in stratigraphic sections along the Rincón Bayo creek (85 m thick) and Camino del Baqueano (at least 182 m thick) at Los Reyunos dam (Fig. 1), and complementary detailed observations of the lower part of the El Imperial Formation were made along the La Horqueta creek.

3.1. Facies association A (*diamictites, conglomerates, and pebbly sandstones*)

3.1.1. Description: This facies association crops out at the base of the El Imperial Formation in the type section (35 m thick) and along La Horqueta creek (18m thick, Figs. 1 and 2). In the El Imperial creek area facies association A comprises massive and stratified diamictites, matrix- and clast-supported conglomerates, pebbly sandstones and scarce levels of shales and fine-grained sandstones bearing disperse dropstones (Fig. 5.1, 5.2 and 5.3). Along La Horqueta creek, matrix- and clast-supported diamictites overlie a low-grade metamorphic basement (Fig. 5.1), forming thick irregular beds (up to 2,5 m thick) and bearing clast of up to 1 meter in maximum diameter (Fig. 5.4). This interval is covered by massive or crudely stratified pebbly mudstones and sandstones, that pass upward to interbedded fine-grained sandstones and shales with dropstones.

In the El Imperial creek area, the lower part of this facies association consists of stacked successions of massive or poorly stratified diamictites and matrix-supported conglomerates, that bear subangular to subrounded clasts up to 20 cm in diameter in a poorly sorted sandy matrix (Fig. 5.3). The clasts are composed of silicified green sandstones, slates, vein quartz, and low-grade schist, all of them derived from the underlying basement. Although subangular shapes predominate, some clasts exhibit subrounded and well-rounded shapes indicating prolonged

Journal Pre-proof

transport; in some cases, occur bullet-shaped (or pentagonal) clasts that exhibit faceted surfaces, and occasional striations.

Upwards, stratified diamictites (Fig. 5.2) and clast-supported conglomerates progressively replace the massive ones. The stratification of the diamictites results from the presence of graded bedding or the existence of a parallel arrangement of the longer axes of the clasts (plane bedding). Clast-supported conglomerates form lenticular beds that frequently pass upward, to low-angle cross-bedded gravelly sandstones. Sporadically, the gravelly sandstones are overlain by thin levels (up to 8 cm thick) of fine-grained sandstones and bioturbated mudstones with root marks, suggest the presence of some levels of paleosols.

3.1.2. Palynological content: Two palynological assemblages have been recovered from this facies association at Arroyo Rincón Bayo (MHNSR-Pal 22, MHNSR-Pal 21). The palynological associations are characterized by palynomorphs of continental origin represented by abundant trilete spores and monosaccate pollen grains in low proportion. The following Pennsylvanian diagnostic species have been recognized: *Anapiculatisporites concinnus* Playford, *Apiculatisporis variornatus* di Pasquo, Azcuy & Souza, *Convolutispora muriornata* Menéndez, *Cristatisporites menendezii* (Menéndez & Azcuy) Playford, *Foveosporites pellucidus* Playford & Helby, *Lundbladispora braziliensis* (Pant & Srivastava) Marques-Toigo & Pons, *Microreticulatisporites punctatus* Knox, *Raistrickia densa* Menéndez, *Vallatisporites ciliaris* (Luber) Sullivan, *Plicatipollenites* spp. and *Potonieisporites neglectus* Potonié & Lele, among others.

3.1.3. Interpretation: The different types of diamictites and matrix-supported conglomerates bearing some faceted and striated clasts, together with the presence of shales with dropstones allow to relate these deposits with the Late Paleozoic Glacial event well recorded in the western basins of Argentina (López Gamundí et al., 1992; López Gamundí, 1987; 2010; Isbell et al., 2012; Limarino et al., 2014). The differences in the proportion and type of diamictites between

Journal Pre-proof

the El Imperial and the Arroyo La Horqueta outcrops probably reflect the proximity to the glacial centers. While in the El Imperial locality no tillite deposit was identified, and most of the diamictites seem to have been originated by gravity flows; in the La Horqueta area, the thick level of massive diamictite covering the basement could result in a till deposit (Fig. 5.1). The stratified diamictites, which are more frequent in the upper part of this facies association in La Horqueta area, would indicate reworking of previous glacial accumulations by gravity flows (Fig. 5.2).

Although the succession is similar in the Arroyo El Imperial, massive diamictites are scarce, and almost all of the material seems remobilized. The lenticular beds of conglomerates and cross-bedded sandstones likely record fluvial sedimentation in braided plains with discrete development of floodplains in which some paleosols developed. The composition of the palynological associations recovered from this interval, formed by terrestrial species and lacking marine palynomorphs, confirms the proposed continental environment.

3.2. Facies Association B (interbedded sandstones and mudstones)

3.2.1. Description: This facies association is divided into two intervals, the lower begins with a thin and laterally persistent level of dark green shales (up to 50 cm thick) that bears abundant dropstones (up to 15 cm in diameter), and poorly preserved plant remains. This interval is followed by interbedded sandstones and mudstones stratified in centimetre-scale beds, with scarce dropstones up to 10 cm in maximum diameter. The top of the lower interval is marked by shales forming a monotonous succession up to 2 m thick, in which dropstones are missing (Fig. 6.1).

The upper interval of this facies association comprises rhythmically stratified fine-grained sandstone and mudstone beds, forming metric-scale coarsening- and thickening upward cycles. The lower part of these cycles is formed by laminated or less frequently massive mudstones stratified in tabular beds up to 20 cm thick, that exhibit bilobate tracks on the top of some beds. The mudstone interval is covered by greenish-gray to yellowish-gray medium- and fine-grained

Journal Pre-proof

sandstones showing horizontal and ripple cross-lamination. Ripple cross-lamination was divided into two types, on the one hand, those showing concave-up sets boundaries, offshoot geometry of the laminae and chevron structures; this type would have resulted of oscillatory flows related to wave action. On the other hand, ripple cross-lamination formed by parallel planar boundaries of sets. In this last case, the presence of unidirectional dip of laminae and lack of chevron disposition of laminae are indicative of unidirectional flows. In some levels, flaser and lenticular bedding are present (Fig. 6.2).

Pebbly sandstones, intercalated at the top of some cycles, appear in low proportion, forming thin irregular and massive beds, bearing clasts up to 3 cm in diameter. The matrix is usually muddy or sandy. Towards the top of the facies association, mudstone beds bear carbonate concretions up to 20 centimetres in diameter.

3.2.2. Palynological content: The localities arroyo El Imperial and Rincón Bayo have provided nine productive samples, MHNSR-Pal 1, 2 (El Imperial creek area), and MHNSR-Pal 23, 24, 25, 26, 27, 28, 29 (Rincón Bayo creek). These palynofloras result more diverse than those found in facies association A, incorporating the presence of *Cordylosporites asperidictyus* (Playford & Helby) Dino & Playford, *Horriditriletes* spp., *Spelaeotriletes triangulus* Neves & Owens, among other trilete spores. Among the pollen grains, specimens of *Limitisporites* and *Circumplicatipollis* are identified. Specimens of apparently monospecific scolecodonts would indicate a shallow marine environment in several of the samples.

3.2.3. Interpretation: The tabular form of the beds, the presence of coarsening and thickening-upwards cycles, the occurrence of wave-ripple cross-lamination and some levels showing flaser and lenticular bedding, suggest that this facies association was deposited under subaqueous conditions (Fig. 6.1 and 6.2). The contact between facies associations A and B is marked by a laterally persistent bed of mudstone that points out the onset of a flooding event. The presence of

Journal Pre-proof

shales with dropstones suggests that the water body was yet in contact with glaciers whose disintegration facilitated the formation of icebergs and the later fall of clasts into the water body. The interval formed by interbedded sandstones and mudstone probably is related to rhythmic alternation of underflow- and overflow-dominated sedimentation while the presence of scarce thin levels of pebbly sandstones suggesting sporadic gravity flows (Holz, 2003; Schatz et al., 2011; Limarino et al., 2014).

The shales at the top of the lower interval probably record a maximum flooding stage, while the lack of dropstones indicates the ultimate glacial retreat from the water body. It is interesting the presence of monospecific scolecodont assemblages that suggest a restricted marine depositional environment (estuary? lagoon?).

The metric-scale coarsening- and thickening upward cycles, which form the middle and upper part of this facies association, correspond to shallowing successions grouped in progradational vertical stacking of cycle sets. This vertical arrangement and the presence of flaser and lenticular lamination suggest that each cycle corresponds to the progradation of mouth bars during high-sea conditions, or the stacking of tidal bars in inner estuary areas (Harris, 1988; Dalrymple and Choi, 2007). The increase in sand/mud ratio towards the top of this facies association probably indicates the transition from the unfilled estuary to a partially filled estuary, similar to the situation described by Harris (1988) and Dalrymple et al. (1992).

3.3. Facies Association C (large- and medium-scale cross-bedded sandstones)

3.3.1. Description: This facies association is composed of whitish-gray, medium- to coarse-grained sandstones, bearing usually higher amounts of quartz grains than lithic fragments, a low proportion of matrix and scarce granule-size clasts dispersed into the sandstones. According to sand size and sedimentary structures, three types of sandstone beds were identified. Firstly, medium- to coarse-grained sandstones that form thick tabular or wedge-shaped beds bearing large-scale cross-bedded sets up to 4 m thick (Figs. 6.3, 7.1). The foresets vary from few

Journal Pre-proof

millimetres to 2 centimetres in thickness and frequently are tangential to the base of the sets. In some cases, thin (few centimetres thick) lenses of gravel (up to 3 cm in diameter) occur at the toes of the foreset. Frequently, lenticular and thin beds of fine-grained sandstones, showing wave-ripple cross-lamination, appear covering the lower part of the foreset, while the top of the cross-bedded sets shows ripple cross-lamination, resulting from the rework by the action of waves or combined flows.

The second type of sandstone, which usually occurs intercalated at the top of the cross-bedded sets described above, corresponds to the stacking of fine-grained sandstones that show horizontal lamination or, less frequently, thin sets of trough cross-bedding. Sporadically, lenticular mudstone beds appear at the top of the stacked successions (Fig. 7.2).

Finally, a third lithological type includes coarse- to medium-grained sandstones that form channelized bodies up to 20 m wide and 1.5 meters thick (Fig. 6.4 and 7.3). In this case, sandstone beds exhibit compound cross-bedding and lateral migration surfaces covered by a thin veneer of mud. In many of these channels, it is possible to recognize two terms, the lower term formed by coarse- or medium-grained massive sandstones with dispersed granules and gravels and the upper term composed of fine-grained sandstones with frequent heterolithic (flaser) and current-ripple cross-lamination.

Paleocurrent directions show two different orientations according to the analyzed type of set, on the one hand coarse-grained sandstones forming the large-scale sets show directions towards the north-east and east-north-east (vector azimuths between 25° and 80°) while axes of the channels and medium-scale cross-bedded units exhibit a west orientation (vectors azimuths between 295° and 250°).

3.3.2. Palynological content: Palynological assemblages have not been recovered for this facies association.

Journal Pre-proof

3.3.3. Interpretation: The large-scale cross-bedded sets are interpreted as littoral bar deposits which were widely influenced by wave action, the lack of mud drapes, reverse flowing ripples and other evidence of tidal currents, point out that the tide had limited participation in the transport of sediments (Visser, 1980; Reading and Collinson, 1986; Hartley and Jolley, 1999) (Figs. 6.3 and 7.1). The horizontal-stratified fine-grained sandstones probably correspond to top bar deposits, while intercalated mudstone beds point out temporary abandonment of the bars, and in some cases, result in bedset-bounding surfaces as described by Eide et al. (2014) (Fig. 7.2). The channelized coarse- to fine-grained sandstones would represent inlet channels related to the estuarine deposits well developed in the facies D (Fig. 7.3).

Paleocurrent measurements allow identifying two different types of bars, on the one hand, sandstones bearing large-scale cross-bedded sets showing paleocurrent directions towards the north-east and east-north-east. In this case, sedimentary structures indicating tidal action are very scarce, and the thickness of cross-bedded sets indicates the development of relatively large bars. This type of deposit is interpreted as wave-dominated bars arrange parallel to the coastline.

On the other hand, the medium-scale cross-bedded sandstones that show foreset dipping west and northwest. These sandstones probably correspond to wave-dominated shoreface bars which were temporarily exposed to rework by tidal currents (heterolithic flaser lamination, mud drapes).

3.4. Facies Association D (laminated mudstones and fine-grained sandstones)

3.4.1. Description: This facies association is composed of interbedded dark-gray mudstones and fine-grained sandstones. Mudstone beds are usually horizontally laminated, rarely massive, frequently show poorly preserved plant remains and abundant bilobate tracks at the top of the beds. The sandstones are fine- to very fine-grained, frequently show high proportions of micaceous minerals (mainly muscovite and biotite in minor amount) and form tabular beds that exhibit abundant heterolithic or horizontal lamination.

Journal Pre-proof

In much smaller proportion appear medium- to coarse-grained sandstones and rarely pebbly sandstones that form channeled bodies of scarce lateral development (less than 3 m) and slightly erosive base. Coarse-grained sandstones and pebbly sandstones are more common in the lower part of the facies, and their presence diminishes vertically up to almost disappear in the middle part. The upper third exhibits two types of medium- to coarse-grained sandstone deposits, a) channelized beds filled with medium- and coarse-grained sand rarely showing low-angle cross-bedding and b) medium-grained ripple-cross laminated sandstones, forming lobate beds with flat bases and concave-up tops.

A remarkable aspect of this facies, in the Arroyo El Imperial section, is the changes in the vertical arrangement of beds. In the lower third, mudstones and sandstones made up finning- and thinning-up successions predominate, which pass in the middle part to highly bioturbated mudstone showing thin intercalations of fine- and very fine-grained sandstones. In the upper third, predominate coarsening- and thickening-up successions formed by fine-grained sandstones at the base and medium- to coarse-grained sandstones; in some cases, gravelly sandstones, at the top of the cycles. Scarce thin levels of carbonaceous mudstones occur intercalated at the top of the sandstone succession.

Although facies association D overlies facies association C, a lateral passage between the lowermost levels of facies D and the top of the facies C have also been observed.

3.4.2. Palynological content: The type locality has provided several palynological assemblages (nine in total), MHNSR-Pal 3, 4, 5, 6, 7, 16, 17, 18, 19, 20 (the last two from the Arroyo Seco de los Potrillos creek). The recovered palynological associations present greater participation of monosaccate pollen accompanying the trilete spores and the first appearance of pollen taeniate represented by *Protohaploxypinus* specimens (MHNSR-Pal MHNSR-Pal 4). A wide diversity of scolecodonts is recognized in deposits with heterolithic lamination. While, in the Rincón Bayo creek, only one sample (MHNSR-Pal 30), from the upper part of the section, contains acritarchs

Journal Pre-proof

of marine origin, instead of scolecodonts, *Protohaploxypinus amplus* (Balme & Hennelly) Hart and the first appearance of the spore *Raistrickia cephalata* Bharadwaj, Kar & Navale, reported in Moscovian assemblages of the Amazonas Basin (Playford and Dino, 2000).

3.4.3. Interpretation: This facies association is interpreted as the product of sedimentation in lagoonal or estuarine environments. Among the main criteria that lead to this interpretation are the dominance of fine-grained sediments (mud and fine-grained sand), frequent heterolithic lamination, abundant bioturbation at some levels, wide diversity of scolecodonts and some acritarchs, together with poorly preserved plant remains (Nichols and Biggs, 1985; Allen, 1991; Dalrymple et al., 1992; Milli et al., 2013).

Moreover, the lack of evaporite levels, the absence of mud cracks, flooded paleosols, or other evidence of subaerial exposition suggest that these deposits correspond to the barred open estuaries in the terminology of Cooper (2001). This type of estuaries is wave-dominated and commonly shows subtidal bars and longshore bars in the outer region.

The lateral passage observed in some cases between the fine-grained rocks of the facies association D and the large-scale cross-bedded sandstones of the facies association C, is common in both modern and ancient estuaries, and indicates the lateral change from sandy longshore bars (outer estuary) to muddy facies (center estuary) with abundant scolecodonts and scarce acritarchs (Dalrymple et al., 1992; Cooper, 2001). During high-sea stage, the filling of the estuary led to the seaward displacement of the mudstones and shales facies belonging to the central estuary, firstly over sandy flood tidal deltas, and then on longshore sandy bars deposits. The result is the formation of finning-upward cycles as those identified in the lower third of this facies association (Nichol et al., 1991; Dalrymple et al., 1992; Lessa et al., 1998; Milli et al., 2013). The medium- to fine-grained sandstones with heterolithic lamination forming channelized beds in the lower third of the facies association are interpreted as tidal inlet channel deposits, which pass laterally to sandstones stratified in tabular beds corresponding to flood-tidal deltas.

Journal Pre-proof

The mudstones and shales with abundant bilobate tracks represent the central part of the estuary, the alternation of bioturbated and non-bioturbed levels probably is related to changes in the fine-grained sediment input. As demonstrated by Nichols and Biggs (1985) and Allen (1991), during a maximum turbidity period, high concentrations of suspended sediments are dispersed as overflows in the estuary, promoting that a large amount of mud and clay be settling avoiding the formation of widespread bioturbation. The presence of abundant scolecodonts in the mudstones and shales indicates low-energy transitional environments, while the scarce acritarchs suggest storms events that introduce microorganisms transported from deeper areas into the water body.

Finally, the coarsening- and thickening-up successions and the coarse-grained sandstones stratified in lenticular beds at the upper third part of this facies association indicate the progradation of mouth bars and subaquatic channels from the neighboring bay-head deltas. The presence of these sediments indicates the partial filling of the estuarine system (Dalrymple et al., 1992; Lessa et al., 1998; Heap et al., 2004) and the transition to the fluvial sedimentation represented in the facies association E.

3.5. Facies Association E (cross-bedded sandstones and conglomerates)

3.5.1. Description: This interval presents very different characteristics to the facies associations previously described since it is formed by coarse-grained sandstones, granule sandstones, and fine-grained conglomerates, as well as two levels of carbonaceous mudstones at the upper part of the facies association. The sandstones and conglomerates, whitish-gray in colour, form lenticular beds, often with channeled geometry, and abundant tabular or trough cross-bedded sets up to 50 cm thick (Fig. 8.1 and 8.2).

According to sedimentary structures and bounding surfaces, two types of architectures were identified in this facies association. The architecture 1 (dominant in the lower part of the facies) results from stacked multistorey channel bodies composed of coarse-grained sandstones and conglomerates forming successions up to 12 m thick. In this case, the geometry of the beds is

Journal Pre-proof

lenticular, the base is strongly erosional, and intercalations of mudstones or fine-grained sandstones are missing (Fig. 8.1).

The architecture 2, which predominates the upper part of the facies association differs from architecture 1 in the development of fining-upward cyclothems (up to 2 m thick), the tabular form of the beds and the presence of mudstones and very fine-grained sandstones at the top of some cycles. Each cyclothem begins with a low- to moderate-relief erosive surface covered by cross-bedded coarse-grained sandstones and gravelly sandstones that include scattered muddy intrabasinal clast. In this interval, compound cross-bedded sets showing lateral accretion surfaces are commonly found (Fig. 8.1).

Coarse-grained sandstones are succeeded by massive medium-grained sandstones that in some cases show thin sets of throughout or tabular cross-bedding. Very fine-grained sandstones and mudstones form the top of the cyclothems, and exceptionally appear carbonaceous mudstones bearing equisetalean plant remains at the top of the facies association (Fig. 8.3).
Paleocurrent measurements were obtained from cross-bedded units of both architecture 1 and 2, although a high dispersion of paleocurrent was obtained, the vector azimuths indicate a southwest direction in the major part of the values (vector azimuths between 190° and 290°).

3.5.2. Palynological content: This facies association could be palynologically characterized only in the Rincón Bayo creek, by the samples MHNSR-Pal 31, 32, 33, 34, 35. The palynofloras are constituted exclusively by palynomorphs of continental origin: trilete spores (e.g., *Raistrickia cephalata, Verrucosisporites menendezii* Gonzalez-Amicón, and monosaccate pollen grains. In the same outcrops plants remains belonging to the *Nothorhacopteris-Botrychiopsis-Ginkgophyllum* Biozone were recovered.

3.5.3. Interpretation: The facies association E marks a significant change in the environmental conditions since it indicates the establishment of a fluvial regime overlying estuaries and lagoons

Journal Pre-proof

deposits of the facies D.

The two types of architectures previously described suggest the presence of at least two types of fluvial systems that very probably records changes in the accommodation space. The lenticular form of the beds, the presence of high-relief erosive surface at the base of the channels, and the lack of fine-grained sediments suggest that architecture 1 probably corresponds to the sedimentation in braided fluvial systems, in which fine-grained floodplains were missing, or they were extremely scarce. The development of stacked multistorey channel deposits probably indicates low-accommodation space conditions that seemingly predominated during the lower half of this facies association (Wright and Marriott, 1993; Tedesco et al., 2010). The lack of lateral accretion bounding surfaces indicates the predominance of fixed channels, in which bars were dominated by downstream-accretion (Miall, 1985, 2006; Skelly et al., 2003).

On the contrary, the development of fining-upward cyclothems, the tabular form of the beds, the presence of lateral accretion surfaces and the fine-grained floodplain deposits in the architecture 2 suggest that the channels showed a higher degree of lateral migration than those that formed the architecture 1. It is important to consider that not all cyclothems show overbank fine-grained deposits at the top, this may be due to the complete erosion of the floodplains before the location of a new channel belt. Another possibility, which seems to be more likely, is that this fluvial system corresponds to a wandering type, rather than a classical meandering river, and therefore the development of fine-grained floodplains was more limited.

The alternation of the architectures 1 and 2 (Fig. 8.1) not only shows changes in the type of the fluvial systems but also records variations in the accommodation space, probably linked to the unstable sea-level position during the late Carboniferous (López Gamundí, 1989, 2010; Limarino et al., 2002). Indeed the best development of floodplains deposits occurs some meters below of the marine transgression of the facies association G.

3.6. Facies Association F (coarsening-upward shale-sandstone cycles)

Journal Pre-proof

3.6.1. *Description*: This facies association is the thickest in the type section (393 m) and is composed of sandstones and mudstones grouped in coarsening-upward cycles. Conglomerates and very coarse-grained sandstones are missing, although scarce levels of coarse-grained sandstones appear at the top of some cycles.

For a better description, the facies association is divided into three sections. The lower one, about 35 m thick, begins with yellowish-gray, fine-grained sandstones, dominated by horizontal or low-angle cross-bedded sets (Fig. 9.1), together with some levels of heterolithic laminated sandstones (mainly flasser type) and thin beds of carbonaceous mudstones. This interval is covered by medium- to fine-grained sandstones showing horizontal or ripple-cross lamination, together with scarce cross-bedded sandstones forming sets up to 15 cm thick. Finally, the top of the lower section is composed of gray laminated mudstones and horizontal-laminated very fine-grained sandstones, all of them stratified in tabular beds (Fig. 10.1).

The middle section, which forms most of the facies association, corresponds to the stacking of coarsening-upward cycles, which range from 9 to 15 m in thickness (Fig. 9.3). In broad terms, each cycle can be divided into four intervals; the lower comprises shales overlying a flooding surface, frequently mudstones show horizontal and vertical bioturbation. The second interval corresponds to horizontal-laminated fine-grained sandstones, with scarce intercalations of mudstones, which are succeeded by wave- and current-ripple cross-laminated sandstones showing in some cases heterolithic lamination (third interval). Finally, the top of the cycle is composed of cross-bedded medium-grained (rarely coarse-grained) sandstones in some cases with scattered granules (Fig. 9.2).

The upper section of this facies association corresponds to a thickening- and coarsening-upwards cycle in which there is a progressive increase in the proportion of sandstones respect to mudstones, these last almost disappear in the upper terms of the facies. The sandstones increase the grain size progressively, at the base predominates thin beds of fine- and very fine-grained laminated sandstones interbedded with mudstone beds, which upwards are replaced by medium-

Journal Pre-proof

grained sandstones, and then, at the top of the facies, the coarse-grained sandstones are dominant. In some cases, the fine-grained sandstones show both hummocky and swaley structures, while in the medium- and coarse-grained sandstones cross-bedded stratification is very common. Besides, some coarse-grained sandstones that form lobate beds preserve remains of trunks and gravel scattered at the top of the strata.

3.6.2. Palynological content: Palynological assemblages were only recovered in the type section, MHNSR-Pal 8, 9 and 10. As a key biostratigraphic species, is identified the presence of the monolete spore *Laevigatosporites vulgaris* (Ibrahim) Ibrahim emend. Alpern & Doubinger, with a significant world presence from the late Bashkirian.

3.6.3. Interpretation: The facies association F records the sea-level changes occurred during the latest Carboniferous and the Early Permian in the western basins of Gondwana. The fine-grained sandstones that form the basal 35m of the facies association, and the thin levels of carbonaceous mudstones intercalated, indicate the beginning of a marine transgression that quickly flooded the fluvial systems of the facies E. In this way, the dominance of low-angle cross-bedded sandstones (Fig. 9.1), closely associated with carbonaceous mudstones, marks the onset of the fluvial valley flooding, and likely the temporary developments of small estuaries or small bays (Dalrymple et al., 1992; Ta et al., 2002). The dominance of horizontal and low-angle cross-bedded sandstones is common in the upper-flow-regime sand flats of the tide-dominated estuaries while heterolithic deposits and carbonaceous mudstones appear in the adjacent mudflats close to emerged areas (Dalrymple et al., 1992; Dalrymple et al., 2012).

The overlying interval that includes horizontal-laminated fine-grained sandstones, without intercalation of carbonaceous mudstones, suggests the transition from foreshore to upper-shoreface environments (Heward, 1981; Helland-Hansen, 2010). In this context, the horizontal or low-angle lamination corresponds to the swash lamination described by Scott (1992) and Hampson, et al. (2008) while the thin sets of cross-bedded sandstones to small bars developed in

Journal Pre-proof

the upper-shoreface.

The mudstones and fine-grained sandstones at the top of the lower section suggest sedimentation in offshore transition settings, where the alternate of mud and sand reflects periods dominated by settling from suspension (mud) and low-energy bottom currents (sand) (Fig. 10.1). The origin of the bottom currents may reflect periodic changes in the position of the fairweather wave-base, or the development of oscillatory and combined flows linked to post-storm periods (Dumas et al., 2005; Isla et al., 2018).

The stacking of coarsening-upward cycles that form the middle section (Fig. 9.3), indicates progradation induced by high-frequency changes in the sea level, where the basal surface of each cycle marks a flooding surface corresponding to a relative rise in the sea level. Different from mudstones of the lower section, the lack of organic matter in the shales suggests that the fine-grained sediments were deposited away from the shoreline. The upward-coarsening organization of each cycle represents coastal progradation interrupted by a new rise in sea level. Therefore, the coarsening-upward cycles are similar to parasequences as described by Van Wagoner et al. (1987), Arnott (1995), Zecchin and Catuneanu (2013) and Ainsworth et al. (2019) among many others. However, in this paper, we avoided using the term parasequence taking into account that the described cycles are limited to the type section of the El Imperial Formation, being their regional extension yet uncertain.

Finally, the upper section formed by a thickening- and coarsening-upward successions was very probably formed by the progradation of a delta system. The mudstones that form the bottom of the succession would represent prodelta facies that upward pass to fine-grained sandstones corresponding to distal delta front environment in which some beds showing hummocky and swaley structures suggest sporadic storm events. Although as demonstrated by Coleman et al. (1998) the storm events affect the whole of the delta environment, combined flows deposited abundant sand in the lower part of the delta front, and introduce sand by means of turbidity currents or underflows into the prodelta areas (Coleman, 1998; Budillon et al., 2005;

Journal Pre-proof

Pattison, 2005).

Proximal delta front facies corresponds to coarse-grained sandstones bearing disperse granules and imprints of trunks, which are interpreted as proximal mouth bar deposits (Mikes and Geel, 2006).

3.7.Facies Association G (mudstones and sandstones with heterolithic lamination)

3.7.1. Description: A thick interval (95 m thick) of fine- and very fine-grained sandstones, included in the facies association G (Fig. 10.2), covers sharply, the medium- to coarse-grained sandstones of the top of the facies association F (Fig. 11.1). The facies G is characterized by its dark gray colour, the preponderance of fine-grained rocks, the extensive development of heterolithic structures (Fig. 10.3), and the localized presence of swale and hummocky structures (Fig. 10.4).

Shales, poorly-laminated mudstones and scarce carbonaceous mudstones, form thick, up to 5 m thick, tabular intervals, in which some layers appear strongly bioturbated, and others exhibit subspherical concretions up to 30 cm in diameter; thin beds of marls with very scarce bioturbation and millimeter ferruginous horizons also occur sporadically. Closely associated with the shale three different types of deposits occur, firstly, intervals up to 2 m thick formed by a delicate (millimetric) alternation of laminae composed of mud and very fine-grained sand. Secondly, intervals dominated by heterolithic cross-lamination (from flaser to lenticular types, Fig. 10.3) that pass transitionally to the above-described shales. A third type consists of fine-grained sandstones showing ripple cross-lamination characterized by the presence of chevrons and foreset laminae with off-shoots.

A very different type of deposit comprises fine- to medium-grained sandstones exhibiting hummocky and swale structures, these sandstones form tabular beds with groove casts, load casts and rarely gutter casts at the base of some beds. These storm deposits form either isolated levels within the muddy deposits or stacked beds up to 1,5m in thickness.

Journal Pre-proof

3.7.2. Palynological content: From this facies association, palynological assemblages have been recovered in two localities: El Imperial creek (MHNSR-Pal 11, 12, 13, 14, 15) and Camino del Baqueano (MHNSR-Pal 36). In addition to spores (less diverse than in the underlying associations) together with the presence of *Converrucosisporites confluens* (Archangelsky & Gamerro) Playford & Dino, non-taeniate pollen and taeniate pollen *(Protohaploxypinus goraiensis* (Potonié & Lele) Balme, *Vittatina subsaccata* (Samoilovhich) Jansonius), acritarchs of marine origin have been recognized in samples 14 and 36.

3.7.3. Interpretation: This facies association is interpreted as deposited in offshore and transition offshore-nearshore environments.

The dominance of shales and mudstones closely associated with heterolithic cross-laminated fine-grained sandstones, and the presence of hummocky structures, suggest deposition in an offshore environment which was alternatingly dominated by both tide and storm currents. This type of shelf was firstly described by Anderton (1976) and Bryant and Smith (1990), and later Johnson and Baldwin (1996) and Pant and Goswami (2003) used the term wave-storm dominated offshore for describing this type of shelf.

The shales and poorly laminated mudstone that make up the bulk of this facies association were settled from suspension in the inner shelf environments during quiescence periods when neither tidal nor storm currents were energetic enough as transport significative proportions of sediments in the offshore area (Macquaker et al. 2010; Schieber, 2016). The thin levels of marls and mudstones showing carbonate concretions, and scarce bioturbation could correspond to a period of low sedimentation rates in the shelf.

The delicate interlamination of mud and very fine-grained sand probably corresponds to hyperpycnal flows generated during periods of high discharges in the coastal areas. This type of deposit frequently is linked to high supply of fine-grained sediments in neighboring deltas, that generates low-velocity bottom currents in the shelf (Wang et al., 2005; Birgenheier et al., 2017).

Journal Pre-proof

Storm deposits are recorded in the sandstones showing hummocky or swale structures and substratal features as groove casts, load casts (Fig. 10.4) and rarely gutter casts (Aigner and Reineck 1982; Snedden and Nummedal, 1991; Sakar et al., 2002).

The ripple-cross laminated sandstones intercalated in shales are similar to those described by Belderson et al. (1982) in shelf dominated by tidal currents showing moderate to high sand supply. Desjardins et al. (2012) also described ripple-cross laminated sandstones in the tide-dominated sand-sheet complexes, but in this case, ripple-cross lamination appears closely associated with compound cross-stratified beds.

Finally, the heterolithic interval composed of flaser and lenticular laminations (Fig. 10.3) probably corresponds to vertically accreted tidal rhythmites (Mazumder and Arima, 2005; Mallik et al., 2012). The presence of bidirectional cross-lamination in some heterolites and the lack of evidence of subaerial exposition reinforces the interpretation of offshore tidal rhythmites for these deposits (Mallik et al., 2012).

3.8.Facies association H (cross-bedded sandstones and conglomerates)

3.8.1. Description: The base of this facies association is marked by an important incision surface carved into the shales and fine-grained sandstones belonging to the facies association G (Figs. 10.2, 11.1). The incision surface can be followed by some hundreds of meters along the strike of the beds and is floored by gravelly sandstones bearing abundant intraformational clasts of mudstones and sandstones belonging to the underlying facies association G.

The facies association shows a reddish-brown color that contrasts with the rest of the Imperial Formation and is made up by coarse medium-grained sandstones, together with a smaller proportion of conglomerates and pebbly sandstones (Fig. 11.2). A few and thin beds of mudstones appear intercalated into the sandstone levels.

According to width/thickness ratio sandstones and conglomerates form tabular beds (using the terminology of Krynine, 1948) or broad to narrow sheets (classification of Gibling

Journal Pre-proof

2006). Sometimes, the beds (up to 2 m thick) show fining-upwards arrangement, in these cases, the base is composed of gravelly sandstone lenses, and even fine conglomerates bearing well-rounded clasts of sandstones, metamorphic rocks, and quartz up to 10 cm in maximum diameter.

The basal interval is covered by medium- to coarse-grained cross-bedded sandstones, sets are both tabular and trough types up to 80 cm thick. The top of the channel body comprises cross-laminated or massive fine-grained sandstones and rarely massive mudstones. It is worth highlighting the presence of lateral accretion surfaces (third-order bounding surfaces by Miall, 1985) in several of the sandstone beds.

The upper part of this facies association shows some differences with the previously described. Firstly conglomerates and coarse-grained sandstones are missing, replaced by well-sorted fine- to medium-grained sandstones without intercalations of mudstones. Secondly, predominates large-scale cross-bedded sets (more than 2 m thick), which pass vertically to sandstones with horizontal or low-angle cross-lamination. Finally, lateral accretion surfaces are missing as well as erosive surfaces at the base of the beds.

The top of this facies association is unconformably covered by breccias, conglomerates and coarse-grained lithic sandstones of the Cochicó Group. Throughout the contact, exists a discolored zone (up to 1 m thick), which probably indicates exposition and paleoweathering before the deposition of the Cochicó Group

3.8.2. Palynological content: No palynofloras was obtained from this facies association.

3.8.3. Interpretation: The sandstones and scarce conglomerates belonging to this facies association were deposited in multi-channelized sandy systems, in which, the cross-bedded sets represent channel bars. The presence of some lateral migration surfaces, together with the presence of fining-upward cycles and the tabular geometry of some beds, suggest lateral migration of some channels with the probable development of point-bars (Jackson, 1976; Miall,

Journal Pre-proof

1985). The dominance in the upper part of this facies association of well-sorted sandstone bearing large-scale cross-bedded sets could indicate the instauration of a fluvial-eolian interaction environment in which small dunes and fluvial channels coexisted (Langford, 1989; Tripaldi and Limarino, 2008). The incision surface at the base of the facies association H, separates marine deposits (facies association G) from fluvial accumulations (facies association H), and is interpreted as the consequence of a forced regression (Fig. 11.1).

The base of this facies association is marked by an important incision surface carved into the shales and fine-grained sandstones belonging to the facies association G (Figs. 10.2, 11.1). The incision surface can be followed by some hundreds of meters along the strike of the beds and is floored by gravelly sandstones bearing abundant intraformational clasts of mudstones and sandstones belonging to the underlying facies association G.

4. Paleoenvironmental evolution of the El Imperial Formation in its type area

The three sections analyzed in this paper (Figs. 3, 4,12), together with the observations made along the La Horqueta creek (Fig. 1), present an integrated scheme of paleoenvironmental evolution for the unit (Fig. 13). The beginning of the sedimentation, represented in the association of facies A, comprises two different lithological terms genetically related. The most characteristic is the one exposed in the El Imperial creek area and corresponds to sandstones and mudstones bearing dropstones associated with stratified resedimented diamictites (Figs. 5.2, 5.4). The second lithological term is represented in the outcrops along the La Horqueta creek that includes massive and chaotically-stratified diamictites (Fig. 5.1). Both types of deposits record the well-exposed glacial Gondwanic event in the upper Paleozoic basins of South America (López Gamundí, 1989, 1997, Isbell et al., 2003, Holz et al., 2008, Perez Loinaze et al., 2010, Limarino et al. , 2014, Assine et al., 2018), but while the less frequent massive diamictites could have been deposited directly by glacial action (tillites), the stratified diamictites indicate reworked of previous glacial accumulations (Benn et al., 2005, Dallimore and Jmieff, 2010, Limarino et al., 2014b, Alonso

Journal Pre-proof

Muruaga et al. ., 2018). The presence of shales with dropstones reinforce the suggested connection with glacial processes (Fig. 5.4).

The base of the facies association B records the beginning of an important marine transgression (Fig. 13), which is well represented in most of the Late Paleozoic outcrops of Argentina (Limarino et al., 2002, López Gamundí et al., 1989, Isbell et al., 2012). This transgression not only appears as an increase in sea level in the coastal and shelf areas, but also as a flooding of fluvial valleys that originated the formation of fjords and estuarine systems in broad areas of the Late Paleozoic basins (Limarino et al., 2002; Marenssi et al., 2005, Dykstra et al., 2006, Pazos et al., 2007, Henry et al., 2014, Alonso Muruaga et al., 2018). Specifically, the facies association B records the passage from the water body in contact with ice masses (shales with dropstones) to the glacial retreat, evidenced by the complete disappearance of dropstones in the upper terms of the facies association. The presence of bilobate tracks, shales with dropstones, the similar lithological composition, and stratigraphic location, suggest the correlation of the facies association B to the interval of restricted marine facies described by Henry et al. (2014) for the El Imperial Formation close the Atuel Canyon.

The facies association C indicates the progradation of coastal facies (Fig. 13), which led to a progressive increase in the proportion of sandstones deposited in littoral bars (Figs. 6.3 and 7.1), which eventually acted as outer bars of the estuary and fjord systems. Regionally, the progradation exposed in the facies associations C and D would correspond with the sandstones with large-scale cross-bedding mentioned by Limarino et al. (2002) in the Paganzo Basin and with the facies of deltas with preserved clinoforms described by Kneller (2004).

The establishment of a continental regime that pointed out the end of the postglacial transgression is shown in the facies association E (Fig. 13), which was deposited in broad braided fluvial plains (Fig. 8.1). These fluvial systems increased the sinuosity of the channels and the number of floodplain deposits vertically, suggesting an increase in the accommodation space towards the top of the facies association. Pazos et al. (2017) described similar continentalization

Journal Pre-proof

at the lower part of the Cabecera del Cañón Member. The considered continentalization is recorded not only in the San Rafael Basin but also most of the basins of western Argentina (Limarino and Spalletti, 2006, Tedesco et al., 2010).

The facies associations F and G records at least two transgressive events (Figs. 9.3, 13), which would correlate with the marine facies described by Pazos (2017) for the middle and upper part of the Cabecera del Cañón Member. These transgressions extend out of the San Rafael Basin, and probably correspond to the late Pennsylvanian-early Cisuralian transgressions recognized in the Paganzo, Río Blanco and Calingasta-Uspallata basins (Limarino et al., 2006, Gutiérrez and Limarino, 2006, Desjardins et al., 2010, Perez Loinaze, et al., 2014).

Finally, the incision surface that marks the base of the facies association H is interpreted as the result of forced regression (Figs. 11.1, 13), as shown by the irregularly of the surface, the omission of sedimentary facies (fluvial successions directly disposed over offshore and transitional deposits) and the presence of abundant intraformational clasts on the incision surface.

5. Palynological associations

The first palynological studies were carried out in localities near the Atuel River (Azcuy and Gutiérrez, 1985, García, 1987) and Diamante (García and Azcuy, 1987, García, 1990). Azcuy and Gutiérrez (1985) recognized a palynological association represented by the genera *Lundbladispora, Cristatisporites, Vallatisporites,* and *Spinozonotriletes*) and monosaccate pollen grains that they assigned to the late Carboniferous.

Later, García and Azcuy (1987) published the discovery of two associations in the vicinity of the Diamante River and Puesto Agua de las Yeguas site. The lower association was referred to the late Carboniferous and the upper to the early Permian. Successive studies by García (1990, 1995, 1996) provided new palynological information about the unit in the localities of the Atuel Canyon, Zitro Mine, arroyo El Imperial, and Puesto Agua de las Yeguas-Pantanito sites.

The most recent data on palynological studies correspond to Pazos et al. (2007) in the

Journal Pre-proof

Atuel Canyon, who included these palynofloras in the subzone B of the DM Biozone of Argentina (César and Gutierrez, 2001).

In the present work, we obtained 36 palynological associations (21 at the El Imperial creek area, 14 at Rincón Bayo creek and 1 at Camino del Baqueano) from facies associations A, B, D, E, F and G. The different recorded taxa, together with the changes in the abundance of spores and pollen grains allowed to recognize three palynological associations (Table 2). A gradual increase of monosaccate and bisaccate pollen grains is recorded from base to top, together with a greater diversity of grains, accompanied by a decrease in the diversity and abundance of spores.

5.1. Palynological association I. It is recognized in fluvial / glacial deposits and in postglacial transgressive sequences of facies associations A and B and characterized by a high diversity of spores that include: *Anapiculatisporites concinnus , Apiculatisporis variornatus* (Fig. 14.1), *Cyclogranisporites microgranus* Bharadwaj, *Cordylosporites asperidyctius* (Fig. 14.3), *Cristatisporites menendezii*, *Cristatisporites* spp., *Convolutispora ordonezii* Archangelsky & Gamerro, *Convolutispora muriornata, Foveosporites pellucidus, Granulatisporites austroamericanus* Archangelsky & Gamerro, *G. varigranifer* Menendez & Azcuy, *Microreticulatasporites punctatus, Retusotriletes anfractus* Menéndez & Azcuy, *Spelaeotriletes triangulus* (Fig. 14.2), *Lundbladispora riobonitensis* Marques-Toigo & Picarelli, *L. braziliensis*, *Grossusporites microgranulatus* Perez Loinaze & César*i, Vallatisporites arcuatus* (Marques-Toigo) Archangelsky & Gamerro, *V. ciliaris* and *Raistrickia densa* (Fig. 14.4).

The pollen grains recognized in this association are restricted to monosaccate represented by the genera *Cannanoropollis* (Fig. 14.5), *Plicatipollenites*, and *Potonieisporites*. The upper deposits corresponding to postglacial marine facies contain scolecodonts, which are represented by a single morphospecies.

Journal Pre-proof

5.2. Palynological association II. It is represented in facies associations D, E and F and characterized by a higher proportion of pollen grains and a diverse and abundant record of scolecodonts. The composition of the association includes 65% spores, 33.5% pollen grains, and 1.5% taeniate pollen grains. The diversity of spores and pollen is equivalent to the underlying palynological association, although some taxa have their first records in this association, such as *Anapiculatisporites tereteangulatus* (Balme & Hennelly) Playford & Dino, *Apiculiretusispora sparsa* Menéndez & Azcuy, *Brevitriletes cornutus* (Balme & Hennelly) Backhouse, *Convolutispora archangelskyi, Horriditriletes superbus* (Foster) Césari, Archangelsky & Seoane, *Laevigatosporites vulgaris* (Fig. 14.6), *Lophotriletes discordis* Gutiérrez & Césari (Fig. 14.7), *Raistrickia cephalata* (Fig. 14.8), *Spelaeotriletes ybertii* and *Verrucosisporites menendezii*. Some monosaccate pollen grains are incorporated, such as *Circumplicatipollis plicatus* Ottone & Azcuy and *Plicatipollenites trigonalis* Lele. The first record of taeniate pollen is represent by *Protohaploxypinus amplus* (Fig. 14.9). At the base of this association is recognized a great diversity of scolecodonts (Fig. 14.10), that toward the top disappear, and instead appear acritarchs as a marine component.

5.3. Palynological association III. It is registered exclusively in the facies association G, in marine platform deposits and is characterized by an increase in the diversity and abundance of taeniate pollen grains (8.5%), represented by: *Illinites unicus* Kosanke emend. Jansonius & Hill (Fig. 14.11), *I. talchirensis* (Lele & Makada) Azcuy, di Pasquo & Valdivia Ampuero, *Hamiapollenites* sp., *Protohaploxypinus goraiensis, P. amplus, P. microcorpus* (Schaarschmidt) Clarke (Fig. 14.12), *Striatoabieites multistriatus* (Balme & Hennelly) Hart, *Vittatina subsaccata* (Fig. 14.13) and *Vittatina* sp. together with the non-taeniate species *Barakarites rotatus* (Balme & Hennelly) Bharadwaj & Tiwari. The spore diversity is lower than the recognized in underlying associations, and some diagnostic taxa are recorded as *Converrucosisporites micronodosus* (Balme & Hennelly) Playford & Dino, *C. confluens* (Fig. 14.14), *Verrucosisporites andersonii*

Journal Pre-proof

and *V. menendezii*. In this association, scolecodonts are not identified, and marine components are represented by diverse acritarchs such as *Gorgonisphaeridium* spp. (Fig. 14.15), *Veryachium* sp., *Leiosphaeridia* sp.

6. Discussion

The paleoenvironmental interpretations reached in the present study coincide in part with the detailed description made by Espejo (1990,1993) and Espejo and López- Gamundí (1994). These authors recognized four facies associations: glacial marine basal, shallow marine, deltaic, and an upper fluvial association.

Another aspect that must be considered is the regional extension of the disconformity mentioned by Pazos et al. (2017) between the Glacigénico and Cabecera del Cañón members in the Atuel Canyon. These authors discussed changes in the direction of the paleocurrents and composition of the sandstones between both members suggesting a hiatus of approximately five million years (late Kasimovian to the early Gzhelian (Pazos et al., 2017). Although, a sea level fall took place at the base of the facies association E, which correlates with the base of the Cabecera del Cañón Member by Pazos et al. (2017), the evolution of the palynological associations studied in this paper indicates the absence of significant hiatus in sedimentation.

Regarding the age of the unit, the palynological associations described in this paper provide new information, not only on the age of the unit but also on the environmental conditions of the facies associations. The biostratigraphic scheme proposed by Césari and Gutiérrez (2001) includes the *Raistrickia densa-Convolutispora muriornata* (DM) and *Pakhapites fusus-Vittatina subsaccata* (FS) biozones, which were referred by to the Namurian-Stephanian and the earliest Permian, respectively according to the chronostratigraphic scale of that time. Césari et al. (2011), based on U-Pb ages on zircons, performed an update including the DM Biozone in the interval late Serpukhovian-Kasimovian?, and referring Subzone A to late Serpukhovian-early Bashkirian, Subzone B to late Bashkirian and Subzone C to the Moscovian-Kasimovian. Besides, the age of

Journal Pre-proof

the FS Biozone was established in the Gzhelian? - Asselian.

In this way, the palynological association I, which corresponds to the facies associations A and B, represents the glacial and postglacial interval, correlated with Subzone A of the DM Biozone (César and Gutierrez, 2001) due to the dominance of spores accompanied by monosaccate pollen grains and absence of taeniate pollen. Therefore, a late Serpukhovian-early Bashkirian age is suggested for facies associations A and B.

In palynological association II, whose bearing levels correspond to the facies associations D, E and F, the first appearance of taeniate pollen (*Protohaploxypinus amplus*) is recorded in the sample MHNSR-Pal 4. Therefore, the start of Subzone B of the DM Biozone, which is referred to the late Bashkirian, is stratigraphically located in the facies association D. César and Gutiérrez (2001) proposed the separation of subzones B and C, by the presence of marine palynomorphs (scolecodonts and acritarchs) in subzone C, considering as reference section the El Imperial Formation. These authors interpreted that the palynofloras with scolecodonts were located towards the top of the El Imperial Formation. However, a review of the distribution of these marine elements reported by García (1990) and the new data obtained in the present study show that the scolecodonts are already present at more basal levels corresponding to Subzones A and B.

The palynological association II also contains marine elements (acritarchs and scolecodonts) in the facies association D, recognizing the first acritarch record (without scolecodonts) together with *Protohaploxypinus* pollen in the MHNSR-Pal 30 sample. It is important to consider, that this sample was collected in Rincón Bayo creek, away from the estuarine environment suggested by the facies association D in the El Imperial area. Therefore, the presence of scolecodonts or acritarchs responds to paleoenvironmental conditions and is not an adequate element to differentiate biostratigraphic units, in this case, subzones B and C. The increase of taeniate pollen grains together with the presence of *Laevigatosporites vulgaris* (in facies association F) could indicate the beginning of Subzone C.

Journal Pre-proof

Finally, the age of the facies association G is deduced by the presence of palynological association III, which shows similarities with the Biozone *Pakhapites fusus-Vittatina subsaccata* (FS), by the presence of *Vittatina* and other pollen grains. Although recovered palynofloras do not contain one of the key taxa of the biozone (*Pakhapites fusus*), the assignment is proposed due to the presence of *Protohaploxypinus* spp., *Converrucosisporites confluens, Barakarites rotatus* and *Illinites unicus*. The presence of the FS Biozone in the El Imperial Formation is also supported by the recognition of *P. fusus, P. ovatus* and *Hamiapollenites fusiformis* by García (1996) in a sample of the upper section of the unit in levels equivalent to the facies association G.

7. Conclusions

1. The sedimentological analysis of the El Imperial Formation in the type section (Arroyo El Imperial), allowed the identification of 8 facies associations. The facies association A characterizes environments related to glacial processes that include massive diamictites, probably corresponding to tillites in the La Horqueta creek area, stratified diamictites resulted of reworking by gravity flows and shales with dropstones. Massive diamictites predominate in most of the exposures of the facies association A.

2. An important postglacial transgression, which includes the facies associations B, C and D, forms most of the lower section of the El Imperial Formation. In the facies association B, characterized by the presence of fine-grained sandstones and mudstones with dropstones, the conditions of maximum flooding were recorded. The facies association C indicates the progradation of coastal bars, while the D corresponds to transitional environments, as estuaries or lagoons.

3. The facies association E points out a significant change in environmental conditions, marked by a rapid sea level fall and the appearance of fluvial deposits with at least two types of architectural designs. The lower architecture characterizes low-accommodation space conditions while the upper architecture higher accommodation space. The contact between the fluvial

Journal Pre-proof

(association E) and transitional facies (association D) is abrupt throughout the analyzed area.

4. Transgressive deposits comprise the facies associations F and G, which differ in the pattern of beds stacking. While that in F the sandstones and mudstones are mainly grouped in cycles, the association G corresponds to muddy deposits sedimented in marine offshore and transitional environments, with the domain of tidal facies and sporadic events of storms.

5. The incision surface recognized between the facies associations G and H is interpreted as the consequence of a forced regression that temporarily exposed platform deposits. The facies association H, formed by sandstones and conglomerates deposited by multichannel sandy rivers, shows towards the uppermost terms eolian-fluvial interaction deposits.

6. The palynological analysis allowed the identification of 106 species of spores, pollen grains, and algae. Its stratigraphic distribution distinguishes three palynological assemblages for the El Imperial Formation (palynological associations I, II, III). Palynological association I is recognized in glacial and postglacial facies and is correlated with subzone A of the *Raistrickia densa-Convolutispora muriornata* (DM) Biozone. Palynological association II, recognized in shallow marine facies, is correlated with subzones B and C of the DM Biozone. Its lower limit corresponds to the first appearance of pollen grains (*Protohaploxypinus*). Finally, association III is identified in the marine deposits of the facies association G and is characterized by the abundance of taeniate pollen grains. Its comparison with equivalent palynofloras described by García (1996) allows to correlate it with the *Pakhapites fusus-Vittatina subsaccata* (FS) Biozone.

7. The occurrence of scolecodonts in the glacial and postglacial facies associations of the lower section of the El Imperial Formation suggests that the initially proposed boundary between subzones B and C of the DM Biozone would not be adequate for this stratigraphic section.

Acknowledgments. For the valuable collaboration in the field trip to Alejandra Pagani, Marcelo de la Fuente, Arturo Taboada, and César Taboada. To Sebastián Mirabelli, Gustavo Holfeltz and Horacio Tassone for the processing of palynological samples. The Ivars family allowed our

Journal Pre-proof

studies in the Arroyo El Imperial area, and kindly cooperated in everything. This study was financed by the grant PICT 0584 of the Anpcyt.

References

Aigner T. , Reineck H.-E., 1982 Proximality trends in modern storm sands from the Helegoland Bight (North Sea) and their implications for basin analysis. Senckenbergiana maritima, 14, 183–215.

Ainsworth, R. B., McArthur, J. B., Lang, S. C., Vonk, A. J., 2019. Parameterizing parasequences: Importance of shelf gradient, shoreline trajectory, sediment supply, and autoretreat. American Association Petroleum Geology Bulletin, DOI:10.1306/04241918149

Alonso-Muruaga, P. J., Limarino, C. O., Spalletti, L. A., Colombo-Piñol, F., 2018. Depositional settings and evolution of a fjord system during the carboniferous glaciation in Northwest Argentina. Sedimentary Geology 369, 28–45.

Arias, W.E., Azcuy, C.L., 1986. El Paleozoico Superior del Cañón del río Atuel, provincia de Mendoza. Revista de la Asociación Geológica Argentina 41, 262–269.

Arnott, R. W. C., 1995. The parasequence definition; are transgressive deposits inadequately addressed?. Journal of Sedimentary Research, 65, 1–6.

Assine, M. L., de Santa Ana, H., Veroslavsky, G., Vesely, F. F., 2018. Exhumed subglacial landscape in Uruguay: Erosional landforms, depositional environments, and paleo-ice flow in the context of the late Paleozoic Gondwanan glaciation. Sedimentary Geology 369, 1–12.

Azcuy, C.L., Gutiérrez, P.R., 1985. Palinología de sedimentitas carbónicas de la Cuenca San Rafael. Ameghiniana 22(1), 97–109.

Benn, D.I., Kirkbride, M.P., Owen, L.A., Brazier, V., 2005. Glaciated valley landsystems. In: Evans, D.J. (Ed.), Glacial Landsystems. Oxford University Press, pp. 372–406.

Budillon, F., Violante, C., Conforti, A., Esposito, E., Insinga, D., Iorio, M., Porfido, S., 2005. Event beds in the recent prodelta stratigraphic record of the small flood-prone Bonea Stream

Journal Pre-proof

(Amalfi Coast, Southern Italy). Marine geology, 222, 419–441.

Césari, S.N., Gutiérrez, P. R., 2001. Palynostratigraphy of Upper Paleozoic sequences in Central-Western Argentina. Palynology 24, 113–146.

Césari, S.N., Limarino, C.O., Gulbranson, E.L., 2011. An Upper Paleozoic biochronostratigraphic scheme for the western margin of Gondwana. Earth-Science Reviews 106, 149–160.

Coleman, J. M., Roberts, H. H., Stone, G. W., 1998. Mississippi River delta: an overview. Journal of Coastal Research 14, 698–716.

Cooper, J. A. G., 2001. Geomorphological variability among microtidal estuaries from the wave-dominated South African coast. Geomorphology. 40, 99–122.

Dallimore, A., Jmieff, D., 2010. Canadian west coast fjords and inlets of the NE Pacific Ocean as depositional archives. In: Howe, J.A., Austin, W.E.N., Forwick, M., Paetzel, M. (Eds.), Fjord Systems and Archives. Geological Society, London, Special Publications. 344, pp. 143–162.

Dalrymple, R. W., Choi, K., 2007. Morphologic and facies trends through the fluvial–marine transition in tide-dominated depositional systems: a schematic framework for environmental and sequence-stratigraphic interpretation. Earth-Science Reviews, 81(3-4), 135–174.

Dalrymple, R. W., Zaitlin, B. A., Boyd, R., 1992. Estuarine facies models; conceptual basis and stratigraphic implications. Journal of Sedimentary Research, 62(6), 1130–1146.

Dalrymple, R. W., Mackay, D. A., Ichaso, A. A., Choi, K. S., 2012. Processes, morphodynamics, and facies of tide-dominated estuaries. In: Davis Jr., R. A., Dalrymple, R. W. (Eds.), Principles of tidal sedimentology, pp. 79-107. Springer.

Desjardins, P. R., Buatois, L. A., Mángano, M. G., Limarino, C.O., 2010. Ichnology of the latest Carboniferous–earliest Permian transgression in the Paganzo Basin of western Argentina: the interplay of ecology, sea-level rise, and paleogeography during postglacial times in Gondwana. Late Paleozoic glacial events and postglacial transgressions in Gondwana. Geological Society of America Special Paper 468, 175–192.

Journal Pre-proof

Dessanti, R.N., 1945. Sobre el hallazgo del Carbónico marino en el arroyo El Imperial de la sierra Pintada (dto. de San Rafael, prov. de Mendoza). Notas del Museo de La Plata, Geología 10(42), 205–220.

Dessanti, R.N., 1956. Descripción geológica de la Hoja 27c-cerro Diamante (Provincia de Mendoza). Boletín de la Dirección Nacional de Minería, 85, 1–79.

Dumas, S., Arnott, R.W.C., Southard, J.B., 2005. Experiments on oscillatory-flow and combined flow bed forms: implications for interpreting parts of the shallow marine rock record. Journal of Sedimentary Research 75, 501–513.

Dykstra, M., Kneller, B.,Milana, J.P., 2006. Deglacial and postglacial sedimentary architecture in a deeply incised paleovalley-paleofjord; the late Carboniferous (Pennsylvanian) Jejenes Formation, San Juan, Argentina. Geol. Soc. Am. Bull. 118, 913–937.

Eide, C. H., Howell, J., Buckley, S., 2014. Distribution of discontinuous mudstone beds within wave-dominated shallow-marine deposits: Star Point Sandstone and Blackhawk Formation, Eastern Utah. AAPG bulletin, 98(7), 1401–1429.

Espejo, I. S., 1990. *Análisis estratigráfico, paleoambiental y de proveniencia de la formación El Imperial, en los alrededores de los ríos Diamante y Atuel, provincia de Mendoza*. Doctoral Thesis, Facultad de Ciencias Exactas y Naturales. Universidad de Buenos Aires.

Espejo, I.S., 1993. Reordenamiento de la estratigrafía neopaleozoica en el sector norte de la Cuenca San Rafael. 12° Congreso Geológico Argentino y 2° Congreso de Exploración de Hidrocarburos, Actas 2, 57–62. Mendoza.

Espejo, I.S., López-Gamundí, O.R., 1994. Source versus depositional controls on sandstone composition in a foreland basin: The El Imperial Formation (mid Carboniferous- lower Permian), San Rafael basin, Western Argentina. Journal of Sedimentary Research, 64(1), 8–16.

Espejo, I.S., Andreis, R.R., Mason, N., 1996. Cuenca San Rafael. En Archangelsky, S. (Ed.*) El Sistema Pérmico en la República Argentina y en la República Oriental del Uruguay*. Academia Nacional de Ciencias Córdoba, Argentina, pp. 163–173.

Journal Pre-proof

Forbes, D. L., 2019. Arctic Deltas and Estuaries: A Canadian Perspective. In Coasts and Estuaries (pp. 123-147). Elsevier.

García, G. B., 1987. Miosporas neopaleozoicas en la Formación El Imperial, en las proximidades de Embalse Valle Grande, Provincia de Mendoza. Proyecto 211, 74–75.

García, G.B., 1990. Escolecodontes de la Formación El Imperial (Paleozoico Superior), Cuenca San Rafael, República Argentina. Ameghiniana 27, 29–38.

García, G.B., 1992. *Estudios paleoflorísticos y análisis bioestratigráfico de la Formación El Imperial y otras unidades equivalentes, Paleozoico superior de la Cuenca San Rafael, Provincia de Mendoza, República Argentina*. Doctoral Thesis, Facultad de Ciencias Exactas y Naturales, Universidad de Buenos Aires

García, G.B., 1995. Palinología de la Formación El Imperial, Paleozoico Superior, Cuenca San Rafael, Argentina. Parte I: Esporas. Ameghiniana 32(4), 315–339.

García, G.B., 1996. Palinología de la Formación El Imperial, Paleozoico Superior, Cuenca San Rafael, República Argentina. Parte II: granos de polen, incertae sedis, acritarcas. Ameghiniana 33(1), 7–33.

García, G.B., Azcuy, C.L., 1987. Dos asociaciones palinológicas de la Formación El Imperial, al sur del río Diamante, provincia de Mendoza, República Argentina. 7º Simposio Argentino de Paleobotánica y Palinología, pp. 59–62.

Gibling, M. R. (2006). Width and thickness of fluvial channel bodies and valley fills in the geological record: a literature compilation and classification. Journal of sedimentary Research 76(5), 731–770.

Giudici, A.R., 1971. Geología de las adyacencias del río Diamante al este del cerro homónimo, provincia de Mendoza, República Argentina. Revista de la Asociación Geológica Argentina 26(4), 444–446.

Gutiérrez, P.R., Limarino, C.O., 2006. El perfil del sinclinal del Rincón Blanco (noroeste de La Rioja): el límite Carbonífero-Pérmico en el noroeste argentino. Ameghiniana, 43(4), 687–703.

Journal Pre-proof

Hampson, G.J., Rodriguez, A.B., Storms, J.E.A., Johnson, H.D., Meyer, C.T., 2008, Geomorphology and high-resolution stratigraphy of wave-dominated shoreline deposits: impact on reservoir-scale facies architecture. In Hampson, G.J., Steel, R.J., Burgess, P.M., Dalrymple, R.W. (Eds.), Recent Advances in models of siliciclastic shallow-marine stratigraphy: SEPM, Special Publication 90, 117–142.

Harris, P.T., 1988. Large scale bedforms as indicators of mutually evasive sand transport and the sequential infilling of wide-mouthed estuaries. Sedimentary Geology 57, 273–298.

Hartley, A. J., Jolley, E. J., 1999. Unusual coarse, clastic, wave-dominated shoreface deposits, Pliocene to middle Pleistocene, northern Chile; implications for coastal facies analysis. Journal of Sedimentary Research, 69(1), 105–114.

Helland□Hansen, W., 2010. Facies and stacking patterns of shelf□deltas within the Palaeogene Battfjellet Formation, Nordenskiöld Land, Svalbard: implications for subsurface reservoir prediction. Sedimentology, 57(1), 190–208.

Henry, L.C., Isbell, J.L., Limarino, C.O., 2014. The late Paleozoic El Imperial Formation, western Argentina: Glacial to post-glacial transition and stratigraphic correlations with arc-related basins in southwestern Gondwana. Gondwana Research 25(4), 1380–1395.

Heward, A.P., 1981. A review of wave-dominated clastic shore-line deposits.- Earth-Science Reviews, 17, 223–276.

Holz, M., 2003. Sequence stratigraphy of a lagoonal estuarine system—an example from the lower Permian Rio Bonito Formation, Paraná Basin, Brazil. Sedimentary Geology, 162(3-4), 305–331.

Holz, M., Souza, P. A., Iannuzzi, R., Fielding, C. R., Frank, T. D., Isbell, J. L., 2008. Sequence stratigraphy and biostratigraphy of the Late Carboniferous to Early Permian glacial succession (Itararé Subgroup) at the eastern-southeastern margin of the Paraná Basin, Brazil. Resolving the late Paleozoic ice age in time and space: Geological Society of America Special Paper 441, 115–129.

Journal Pre-proof

Isbell, J.L., Miller, M.F., Wolfe, K.L., Lenaker, P.A., 2003. Timing of late Paleozoic glaciation in Gondwana: was glaciation responsible for the development of northern hemisphere cyclothems? In: Chan, M.A., Archer, A.W. (Eds.), Extreme Depositional Environments: Mega End Members in Geologic Time. Geological Society of America Special Paper. 370, pp. 5–24.

Isbell, J. L., Henry, L. C., Gulbranson, E. L., Limarino, C. O., Fraiser, M. L., Koch, Z. J., ... Dineen, A. A. 2012. Glacial paradoxes during the late Paleozoic ice age: evaluating the equilibrium line altitude as a control on glaciation. Gondwana research, 22(1), 1–19.

Isla, M. F., Schwarz, E., Veiga, G. D., 2018. Bedset characterization within a wave-dominated shallow-marine succession: an evolutionary model related to sediment imbalances. Sedimentary geology, 374, 36–52.

Jackson, R. G., 1976. Depositional model of point bars in the lower Wabash River. Journal of Sedimentary Research, 46(3), 579–594.

Kneller, B., Milana, J. P., Buckee, C., al Ja'aidi, O., 2004. A depositional record of deglaciation in a paleofjord (Late Carboniferous [Pennsylvanian] of San Juan Province, Argentina): The role of catastrophic sedimentation. Geological Society of America Bulletin 116(3-4), 348–367.

Krynine, P.D., 1948, The megascopic study and field classification of sedimentary rocks: Journal of Geology 56, 130–165.

Langford, R. P., 1989. Fluvial□aeolian interactions: Part I, modern systems. Sedimentology 36(6), 10235.

Lessa, G. C., Meyers, S. R., Marone, E., 1998. Holocene stratigraphy in the Paranagua Bay estuary, southern Brazil. Journal of Sedimentary Research, 68(6), 1060—1076.

Limarino, C. O., Spalletti, L. A. 2006. Paleogeography of the upper Paleozoic basins of southern South America: An overview. Journal of South American Earth Sciences 22(3-4), 134–155.

Limarino, C. O., Césari, S.N., Net, L.I., Marenssi, S.A., Gutiérrez, R.P., Tripaldi A., 2002. The Upper Carboniferous postglacial transgression in the Paganzo and Rıo Blanco basins

Journal Pre-proof

(northwestern Argentina): facies and stratigraphic significance. Journal of South American Earth Sciences 15(4), 445–460.

Limarino, C.O., Césari, S.N., Spalletti, L.A., Taboada, A.C., Isbell, J.L., Geuna, S., Gulbranson, E.L., 2014a. A paleoclimatic review of southern South America during the late Paleozoic: A record from icehouse to extreme greenhouse conditions. Gondwana Research 25(4), 1396–1421.

Limarino, C. O., Alonso-Muruaga, P. J., Ciccioli, P. L., Loinaze, V. S. P., Césari, S. N., 2014b. Stratigraphy and palynology of a late Paleozoic glacial paleovalley in the Andean Precordillera, Argentina. Palaeogeography, Palaeoclimatology, Palaeoecology, 412, 223–240.

López Gamundí, O.R., 1987. Depositional models for the glaciomarine sequences of Andean Late Paleozoic basins of Argentina. Sedimentary Geology, 52, 109–126.

López Gamundi, O.R., 1989. Postglacial transgressions in late Paleozoic basins of western Argentina: a record of glacioeustatic sea level rise. Palaeogeogr. Palaeoclimatol. Palaeoecol. 71, 257–270.

López Gamundí, O.R., 1997. Glacial-postglacial transition in the Late Paleozoic basins of southern South America. In: Martini, I.P. (Ed.), Late Glacial and Postglacial Environmental Changes-QuaternaryCarboniferous-Permian, and Proterozoic. Oxford, Oxford University Press, pp. 147–168.

López-Gamundí, O.R., 2010. Transgressions related to the demise of the Late Paleozoic Ice Age: Their sequence stratigraphic context. Geological Society of America Special Papers, 468, 1–35.

López-Gamundí, O. R., Limarino, C. O., Cesari, S. N., 1992. Late Paleozoic paleoclimatology of central west Argentina. Palaeogeography, Palaeoclimatology, Palaeoecology, 91, 305–329.

Marenssi, S.A., Tripaldi, A., Limarino, C.O., Caselli, A.T., 2005. Facies and architecture of a carboniferous grounding-line system from the Guandacol Formation, Paganzo Basin, Northwestern Argentina. Gondwana Research 8, 187–202.

Miall, A. D., 1985. Architectural-element analysis: a new method of facies analysis applied to fluvial deposits. Earth-Science Reviews 22(4), 261–308.

Journal Pre-proof

Miall, A. D., 2006. Reconstructing the architecture and sequence stratigraphy of the preserved fluvial record as a tool for reservoir development: A reality check. AAPG bulletin, 90(7), 989–1002.

Mikes, D., Geel, C. R., 2006. Standard facies models to incorporate all heterogeneity levels in a reservoir model.Marine and Petroleum Geology 23, 943–959.

Milli, S., D'Ambrogi, C., Bellotti, P., Calderoni, G., Carboni, M. G., Celant, A., Pichezzi, R. M., 2013. The transition from wave-dominated estuary to wave-dominated delta: the Late Quaternary stratigraphic architecture of Tiber River deltaic succession (Italy). Sedimentary Geology, 284, 159–180.

Nichols, M. M., Biggs, R. B., 1985. Estuaries. In: Davis R. A. (Ed.) Coastal Sedimentary Environments (2 ed.), Springer-Verlag, pp. 77-186

Nichols, M.M., Johnson, G.H., Peebles, P.C., 1991, Modern sediments and facies model for a microtidal coastal plain estuary, the James estuary, Virginia: Journal of Sedimentary Petrology, 61, 883–899.

Pattison, S. A., 2005. Storm-influenced prodelta turbidite complex in the lower Kenilworth Member at Hatch Mesa, Book Cliffs, Utah, USA: implications for shallow marine facies models. Journal of Sedimentary Research, 75(3), 420–439.

Pazos, P.J., 2002. Palaeoenvironmental framework of the late Palaeozoic glacial to postglacial transition in the Paganzo-Calingasta basin (South America) and Karoo-Kalahari basins (Southern Africa): ichnological implications. Gondwana Research 5, 619–640.

Pazos, P.J., di Pasquo, M., Amenábar, C.R. 2007. Trace fossils of the glacial to postglacial transition in the El Imperial Formation (Upper Carboniferous), San Rafael basin, Argentina. Society for Sedimentary Geology, Special Publication 88, 137–147.

Pazos, P., Rusconi, F., Loss, L., Gutiérrez, C., Heredia, A., 2017. Estratigrafía de la Formación El Imperial (Penssilvaniano y Cisuraliano) en el Cañón del Atuel, Cuenca San Rafael. Revista de la Asociación Geológica Argentina 74(2), 155–162.

Journal Pre-proof

Perez Loinaze, V.S., Limarino, C.O., Césari, S.N., 2010. Glacial events in Carboniferous sequences from Paganzo and Río Blanco Basins (northwest Argentina): palynology and depositional setting. Geol. Acta 8, 399–418.

Perez Loinaze, V. S., Limarino, C. O., Césari, S. N., 2014. Carboniferous outcrops at La Herradura creek, San Juan Province (western Argentina), revisited: age of the transgressions. Andean Geology 41, 83–105.

Playford, G., Dino, R., 2000. Palynostratigraphy of upper Palaeozoic strata (Tapajós Group), Amazonas, Brazil: Part Two. Palaeontographica Abteilung B, 87–145.

Reading, H. G., Collinson, J. D., 1996. Clastic coasts. In Reading, HG,(Ed.), Sedimentary environments: Processes, facies and stratigraphy. Blackwells, Cornwall, 154–231.

Scott, E.S., 1992, The palaeoenvironments and dynamics of the Rannoch– Etive nearshore and coastal succession, Brent Group, northern North Sea, in Morton, A.C., Haszeldine, R.S., Giles, M.R., and Brown, S., eds., Geology of the Brent Group: Geological Society of London, Special Publication 61, 219–238.

Schatz, E. R., Mángano, M. G., Buatois, L. A., Limarino, C. O., 2011. Life in the Late Paleozoic Ice Age: Trace fossils from glacially influenced deposits in a Late Carboniferous fjord of western Argentina. Journal of Paleontology, 85(3), 502–518.

Skelly, R. L., Bristow, C. S., Ethridge, F. G., 2003. Architecture of channel-belt deposits in an aggrading shallow sandbed braided river: the lower Niobrara River, northeast Nebraska. Sedimentary Geology, 158(3-4), 249–270.

Stappenbeck, R., 1934. Geología de la Montaña de San Rafael. Y.P.F.-Informe Inédito.

Ta, T. K.O., Nguyen, V. L., Tateishi, M., Kobayashi, I., Saito, Y., Nakamura, T., 2002. Sediment facies and Late Holocene progradation of the Mekong River Delta in Bentre Province, southern Vietnam: an example of evolution from a tide-dominated to a tide-and wave-dominated delta. Sedimentary Geology, 152(3-4), 313–325.

Tedesco, A., Ciccioli, P., Suriano, J., Limarino, C. O., 2010. Changes in the architecture of fluvial

Journal Pre-proof

deposits in the Paganzo Basin (Upper Paleozoic of San Juan province): an example of sea level and climatic controls on the development of coastal fluvial environments. Geologica acta, 8(4), 463–482.

Tripaldi, A., Limarino, C. O., 2008. Ambientes de interacción eólica-fluvial en valles intermontanos: ejemplos actuales y antiguos. Latin American journal of sedimentology and basin analysis *15*(1), 43–66.

Van Wagoner, J. C., Mitchum Jr, R. M., Posamentier, H. W., Vail, P. R., 1987. Seismic stratigraphy interpretation using sequence stratigraphy: Part 2: Key definitions of sequence stratigraphy. In: Bally A.W. (Ed.) Atlas of seismic stratigraphy, AAPG Studies in Geology 27, 11–14.

Visser, M. J.,1980. Neap-spring cycles reflected in Holocene subtidal large-scale bedform deposits: a preliminary note. Geology, 8(11), 543–546.

Wright, V. P., Marriott, S. B., 1993. The sequence stratigraphy of fluvial depositional systems: the role of floodplain sediment storage. Sedimentary geology, 86(3-4), 203–210.

Zecchin, M., Catuneanu, O., 2013. High-resolution sequence stratigraphy of clastic shelves I: units and bounding surfaces. Marine and Petroleum Geology, 39(1), 1–25

Figure captions:

Figure 1. Map showing the location of the sites mentioned in the text (stars).

Figure 2: Geologic map of the El Imperial creek area. References: FA= Facies association; A-A, B-B: strike section.

Figure 3: Stratigraphic section of the El Imperial Formation in the type locality. For references see figure 4.

Figure 4: Stratigraphic section of the El Imperial Formation in the type locality. See also figure 3.

Figure 5: Characteristics of the diamictites of the facies association A. 1. Massive diamictite (a)

Journal Pre-proof

resting on the methamorphic rocks of the La Horqueta Formation (La Horqueta creek); 2. Crudely stratified diamictite with thin intercalated sandy levels (El Imperial creek); 3. Fine-grained massive diamictite (El Imperial creek); 4 . Dropstone (a) in shales intercalated into the diamictites (La Horqueta creek).

Figure 6. 1. Mudstone and very fine-grained sandstones of the facies association B exhibiting heterolithic-cross lamination (El Imperial creek area); 2. Interlaminated succession of mudstones and fine-grained sandstones showing ripple-cross lamination (facies association B); 3. Large-scale cross-bedded sandstones that characterize marine bars of the facies association C (Rincón Bayo creek); 4. Small channel cutting across deposits of littoral bars of the facies association C (Rincón Bayo creek).

Figure 7: Aspect of different types of deposits belonging to the facies association C at the El Imperial creek area. 1. Stacked large-scale cross-bedded sets corresponding to littoral bars of the facies association C; 2. Fine grained deposits (mudstone), intercalated into the sandy bars of the facies 4, arrows indicate the upward increase in grain-size; 3. Tidal channel (A) cutting across the sandy littoral bar deposit (B) that covers shales and mudstones (C)

Figure 8: 1. General view of the coarse-grained sandstones and conglomerates that form the facies association E, 1 and 2 indicate the two types of fluvial architecture described in the text; 2. Cross-bedded coarse-grained sandstones showing lateral accretion surfaces (arrows, facies association E); 3. Aspect of the top of the facies association E, notice the decrease thickness of the channel and the occurrence of carbonaceous mudstones corresponding to floodplain deposits. All images from the El Imperial creek.

Figure 9: 1. Fine-grained sandstones with ripple-cross lamination, correspondig to shoreface

Journal Pre-proof

deposits of the facies F; 2. Littoral bars deposits of the facies association F composed of cross-bedded sandstones ; 3. General view of the facies association F showing the presence of coarsening-upwards cycles (El Imperial creek).

Figure 10: 1. Shales and mudstones corresponding to offshore deposits of the facies F; 2. Upper contact between facies G and H, note the irregular surface (incision, arrows) at the base of the facies H; 3. Interbedded shales and fine-grained sandstones showing heterolithic lamination (facies H); 4. Hummocky cross-laminated sandstones corresponding to storm deposits intercalated into the muddy offshore deposits of the facies G. All images taken at the El Imperial creek.

Figure 11: 1. General view of the transition among the facies association F,G and H. The black line, at the base of the facies H, points out the irregular topography originated by the incision during the forced sea level fall (El Imperial creek). 2. View of the fluvial sandstones belonging to the facies association H in the quarry. All images taken at the El Imperial creek.

Figura 12. Stratigraphic sections of the sites Camino del Baqueano (A) and Rincón Bayo creek (B) with productive palynological samples.

Figure 13: Synthesis of the paleoenvironmental evolution of the El Imperial Formation and its relation with the sea level changes.

Figure 14. 1. *Apiculatisporis variornatus* di Pasquo, Azcuy & Souza, MHNSR-Pal 21(6) P41/0; 2. *Spelaeotriletes triangulus* Neves & Owens, MHNSR-Pal 28(1) P28/4; 3. *Cordylosporites asperidyctius* (Playford & Helby) Playford, MHNSR-Pal 34(4) N59/4; 4. *Raistrickia densa* Menéndez, MHNSR-Pal 24(1) J35/0; 5. *Cannanoropollis densus* (Lele) Bose & Maheshwari,

Journal Pre-proof

MHNRS-Pal 24(2) Q38/3; 6. *Laevigatosporites vulgaris* (Ibrahim) emend. Alpern & Doubinger, MHNSR- Pal12(1) W60/2; 7.*Lophotriletes discordis,* Gutiérrez & Césari, MHNSR-Pal 14(3) D37/0; 8. *Raistrickia cephalata* Bharadwaj, Kar & Navale, MHNSR-Pal 30(3) Y58/2; 9. *Protohaploxypinus amplus* (Balme & Hennelly) Hart, MHNSR-Pal 30(1) H64/1; 10. Scolecodont indet. MHNSR-Pal 16(3) D24/4; 11. *Illinites unicus* Kosanke emend. Jansonius & Hill, MHNSR-Pal 14(2) Y37/4; 12. *Protohaploxypinus microcorpus* (Schaarschmidt) Clarke, MHNSR-Pal 14(1) M52/0; 13. *Vittatina subsaccata* (Samoilovich) Jansonius, MHNSR-Pal 14(4) Y28/3; 14. *Converrucosisporites confluens* (Archangelsky & Gamerro) Playford & Dino, MHNSR-Pal 13(5) U54/4; 15. *Gorgonisphaeridium* sp. A García, MHNSR-Pal 14(4) M53/2. Scale 20 μm

Table 1. Characterization of facies associations and thickness.

Table 2. Distribution of the main diagnostic palynomorphs.

Journal Pre-proof

Facies Association	Lithology	Interpretation	Thickness
H	*Cross-bedded red sandstones, with smaller proportion conglomerates and mudstones*	*High-sinuosity multi-channel fluvial systems, towards the top, fluvial-aeolian interaction deposits*	60 m
G	*Mudstones, shales and fine-grained sandstones with heterolitic lamination. Sandstone beds showing hummocky cross-lamination*	*Offshore deposits passing upwards to transition offshore-nearshore and coastal environments*	95 m
F	*Fine- and very fine-grained sandstones intercalated with mudstones*	*Transgressive marine succesion mainly deposited in coastal and proximal offshore environments*	393 m
E	*Coarse-grained sandstones, pebbly sandstones and scarce conglomerates showing cross-bedding*	*Fluvial sedimentation in braided (to anastomosing?) fluvial plains*	32 m
D	*Mudstones and very fine-grained sandstones with heterolitic cross-lamination*	*Transitional environments, from estuarine to lagoonal.*	110 m
C	*Stacked sandstone beds showing large-scale cross-bedding and less frequently horizontal lamination*	*Large-scale sandy bars, littoral bars and in some cases mouth bars*	45 m
B	*Interbedded sandstones and mudstones*	*Coastal facies corresponding to the postglacial transgression*	77 m
A	*Diamictites, matrix- and clast-supported conglomerates, pebbly sandstones, fine-grained sandstones and shales with dropstones*	*Lacustrine and fluvial deposits in glacially-influenced environments. Reworked diamictites by gravity flows are frequent.*	48 m

Journal Pre-proof

Species	Association I	Association II	Association III
Anapiculatisporites concinnus	X		
Apiculatisporites variornatus	X		
Apiculiretusispora alonsoi	X		
Foveosporites pellucidus	X		
Granulatisporites varigranifer	X		
Microreticulatisporites punctatus	X		
Spelaeotriletes triangulus	X		
Convolutispora muriornata	X	X	
Cordylosporites asperidictyus	X	X	
Cristatisporites menendezii	X	X	
Raistrickia densa	X	X	
Raistrickia rotunda	X	X	
Scolecodonts	X	X	
Cristatisporites spp.	X	X	X
Cyclogranisporites microgranus	X	X	X
Granulatisporites austroamericanus	X	X	X
Grossusporites microgranulatus	X	X	X
Lundbladispora braziliensis	X	X	X
Plicatipollenites spp.	X	X	X
Potonieisporites spp.	X	X	X
Circumplicatipollis spp.	X	X	X
Crucisaccites spp.	X	X	X
Limitisporites spp.	X	X	X
Divarisaccus stringoplicatus	X	X	X
Caheniasaccites spp.	X	X	X
Canannoropollis spp.	X	X	X
Spelaeotriletes spp.	X	X	X
Vallatisporites spp.	X	X	X
Horriditriletes spp.	X	X	X
Apiculiretusispora sparsa		X	
Raistrickia cephalata		X	
Brevitriletes spp.		X	X
Laevigatosporites vulgaris		X	X
Protohaploxypinus amplus		X	X
Acritarchs		X	X
Converruc.confluens/C. micronodosus			X
Verrucosisporites andersonii			X
Barakarites rotatus			X
Illinites talchirensis			X
I. unicus			X
Platysaccus trumpii			X

Journal Pre-proof

Journal Pre-proof

Protohaploxypinus goraiensis			X
P. microcorpus			X
Striatoabieites multistriatus			X
Vittatina subsaccata			X
Prasinophytes			X

Journal Pre-proof

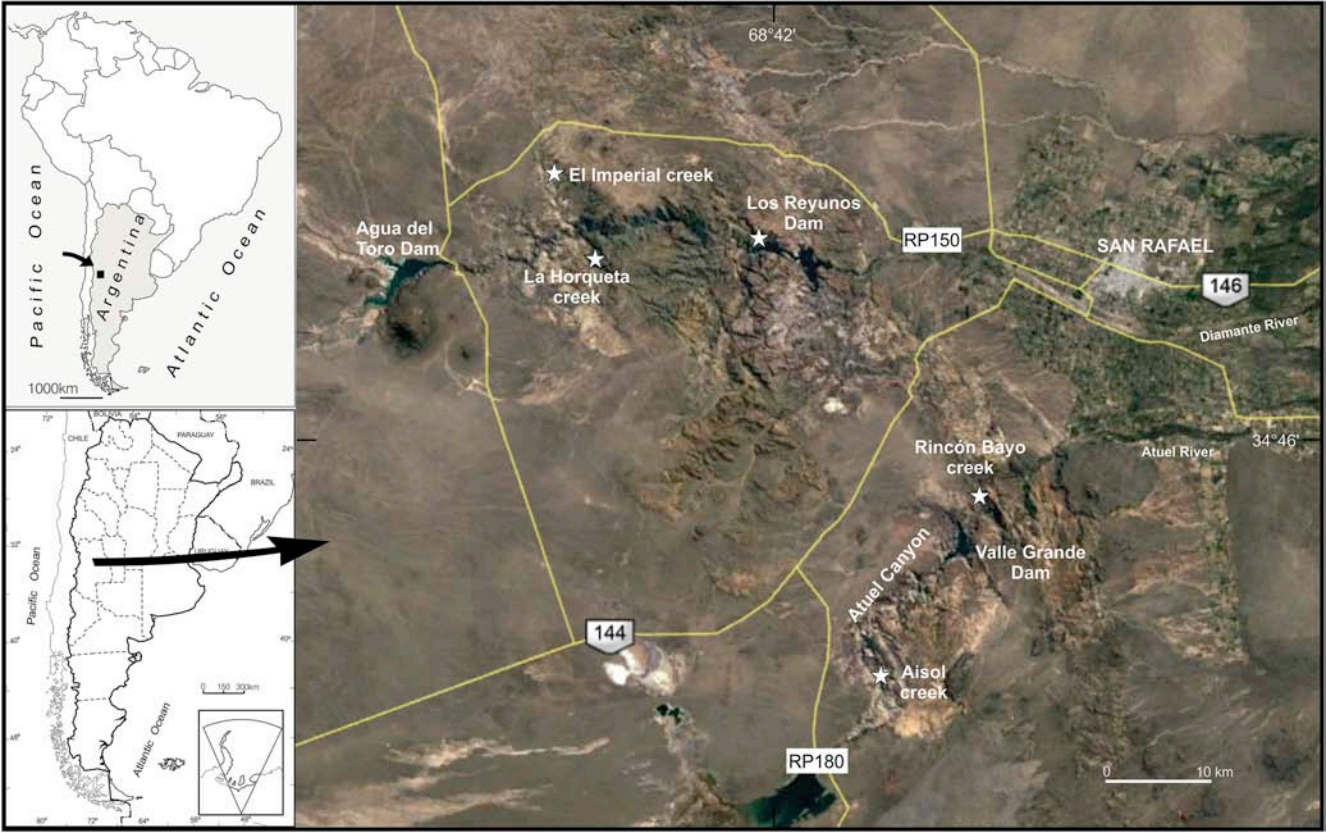
Pacific Ocean
Argentina
Atlantic Ocean
1000km
CHILE
PARAGUAY
BRAZIL
Pacific Ocean
Atlantic Ocean
0 150 300km
68°42'
El Imperial creek
Los Reyunos Dam
Agua del Toro Dam
La Horqueta creek
RP150
SAN RAFAEL
146
Diamante River
34°46'
Atuel River
Rincon Bayo creek
Valle Grande Dam
Atuel Canyon
144
Aisol creek
RP180
0 10 km

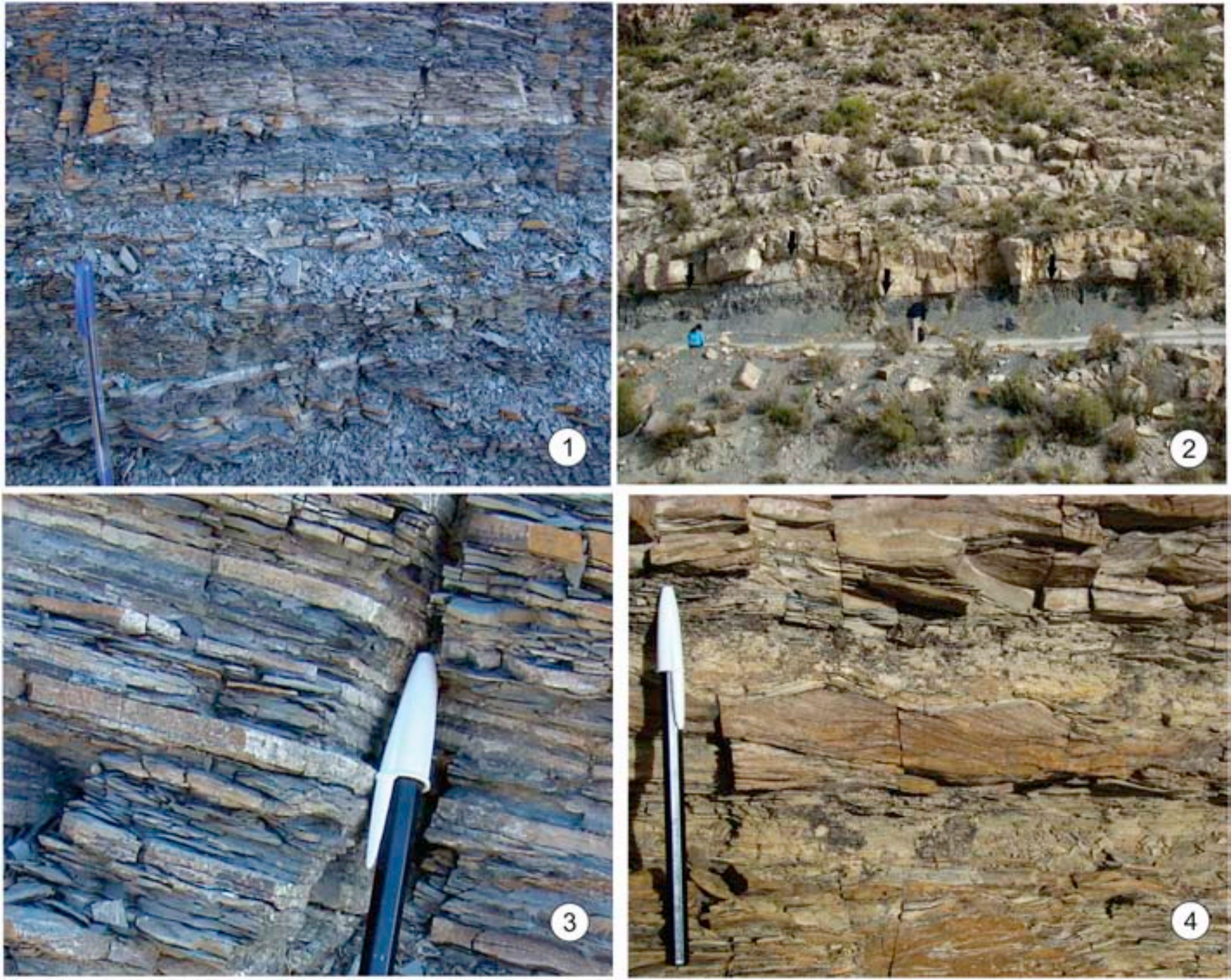
1
2
3
4

H
G
F
1

2

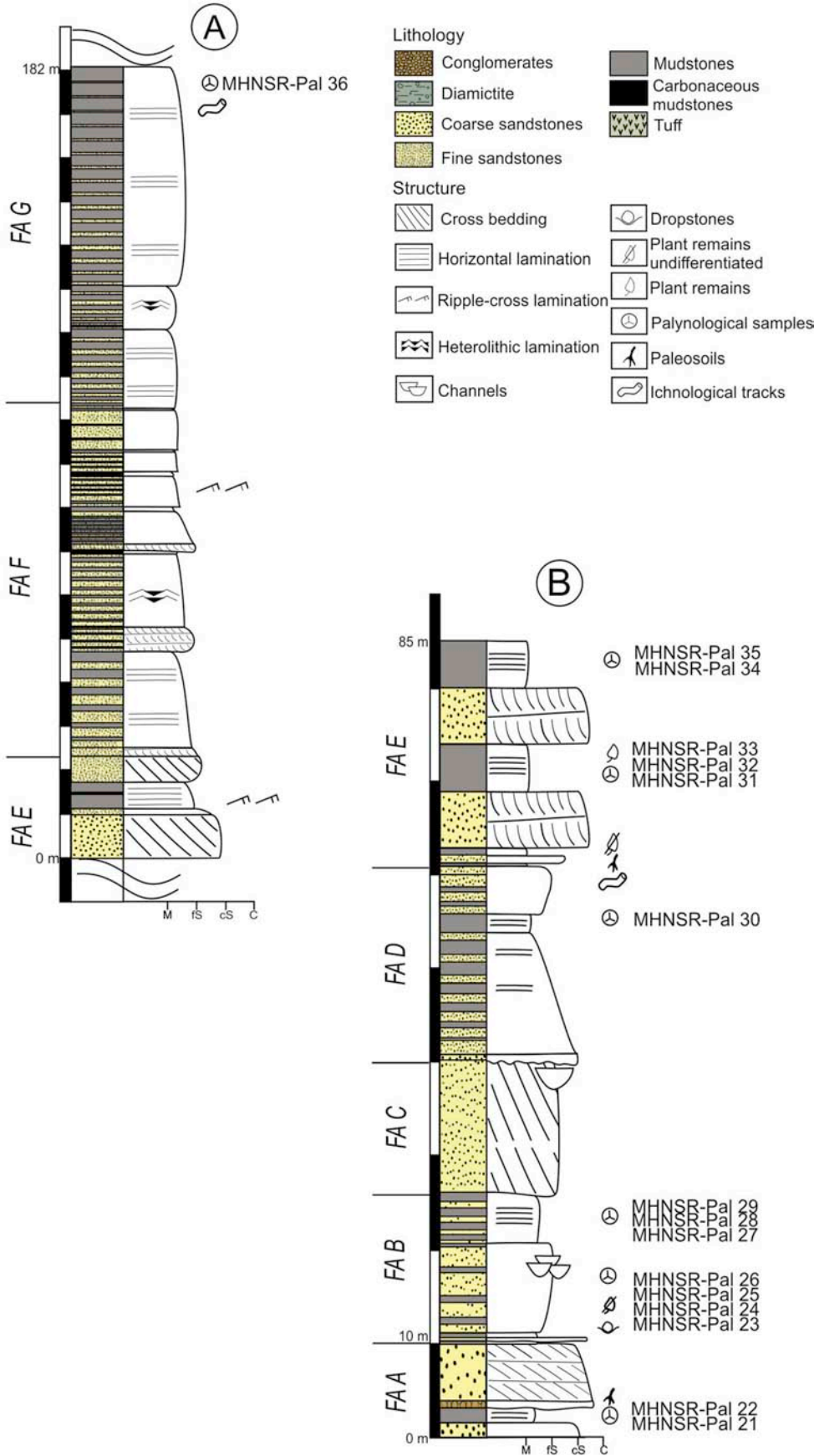
A
182 m
MHNSR-Pal 36
FA G
FA F
FA E
0 m
M
fS
cS
C
Lithology
Conglomerates
Diamictite
Coarse sandstones
Fine sandstones
Mudstones
Carbonaceous mudstones
Tuff
Structure
Cross bedding
Horizontal lamination
Ripple-cross lamination
Heterolithic lamination
Channels
Dropstones
Plant remains undifferentiated
Plant remains
Palynological samples
Paleosoils
Ichnological tracks
B
85 m
MHNSR-Pal 35
MHNSR-Pal 34
MHNSR-Pal 33
MHNSR-Pal 32
MHNSR-Pal 31
MHNSR-Pal 30
MHNSR-Pal 29
MHNSR-Pal 28
MHNSR-Pal 27
MHNSR-Pal 26
MHNSR-Pal 25
MHNSR-Pal 24
MHNSR-Pal 23
MHNSR-Pal 22
MHNSR-Pal 21
FA E
FA D
FA C
FA B
FA A
10 m
0 m
M
fS
cS
C

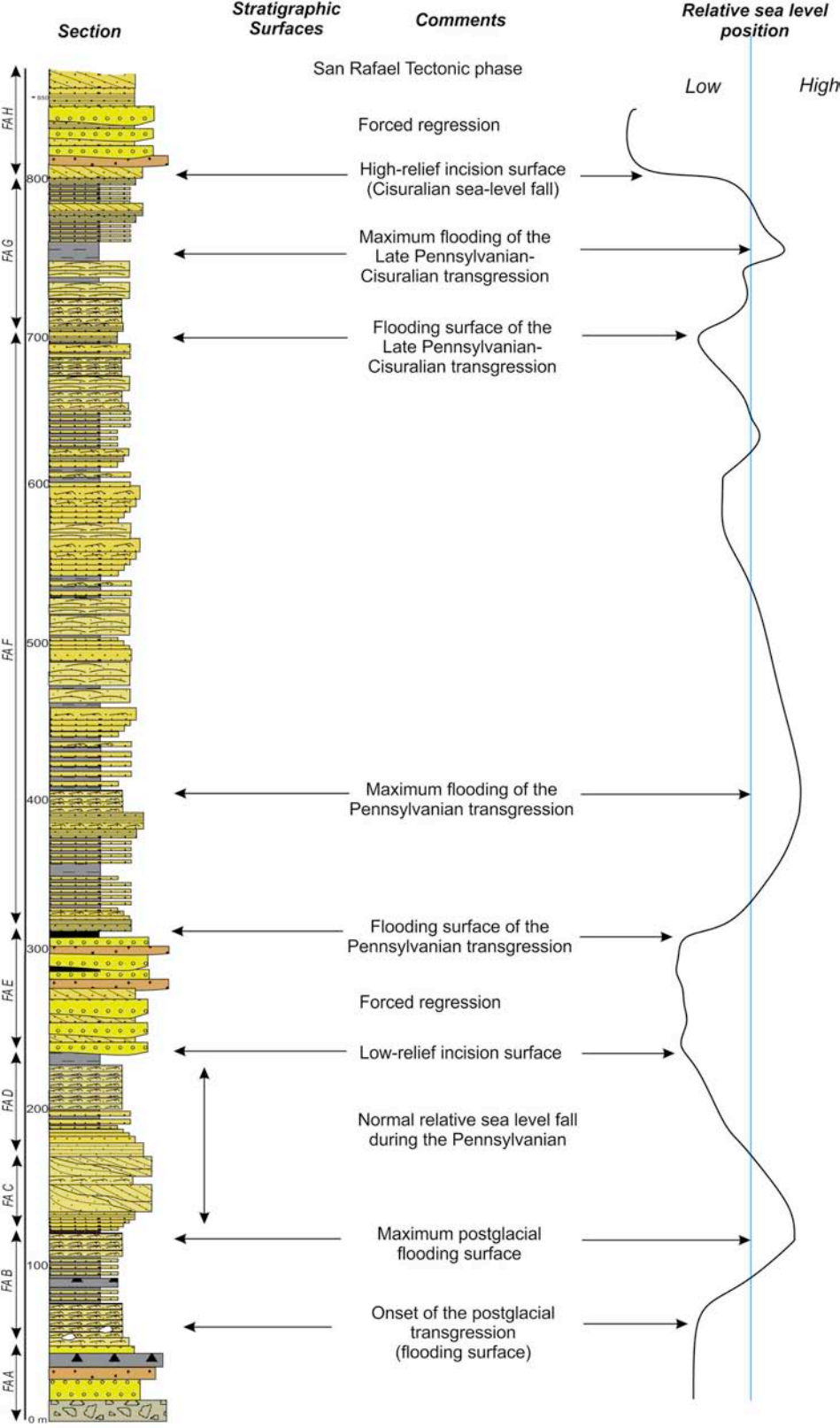
Section
Stratigraphic Surfaces
Comments
Relative sea level position
San Rafael Tectonic phase
Low
High
FA H
FA G
FA F
FA E
FA D
FA C
FA B
FA A
800
700
600
500
400
300
200
100
0 m
Forced regression
High-relief incision surface (Cisuralian sea-level fall)
Maximum flooding of the Late Pennsylvanian-Cisuralian transgression
Flooding surface of the Late Pennsylvanian-Cisuralian transgression
Maximum flooding of the Pennsylvanian transgression
Flooding surface of the Pennsylvanian transgression
Forced regression
Low-relief incision surface
Normal relative sea level fall during the Pennsylvanian
Maximum postglacial flooding surface
Onset of the postglacial transgression (flooding surface)
La Horqueta Fm

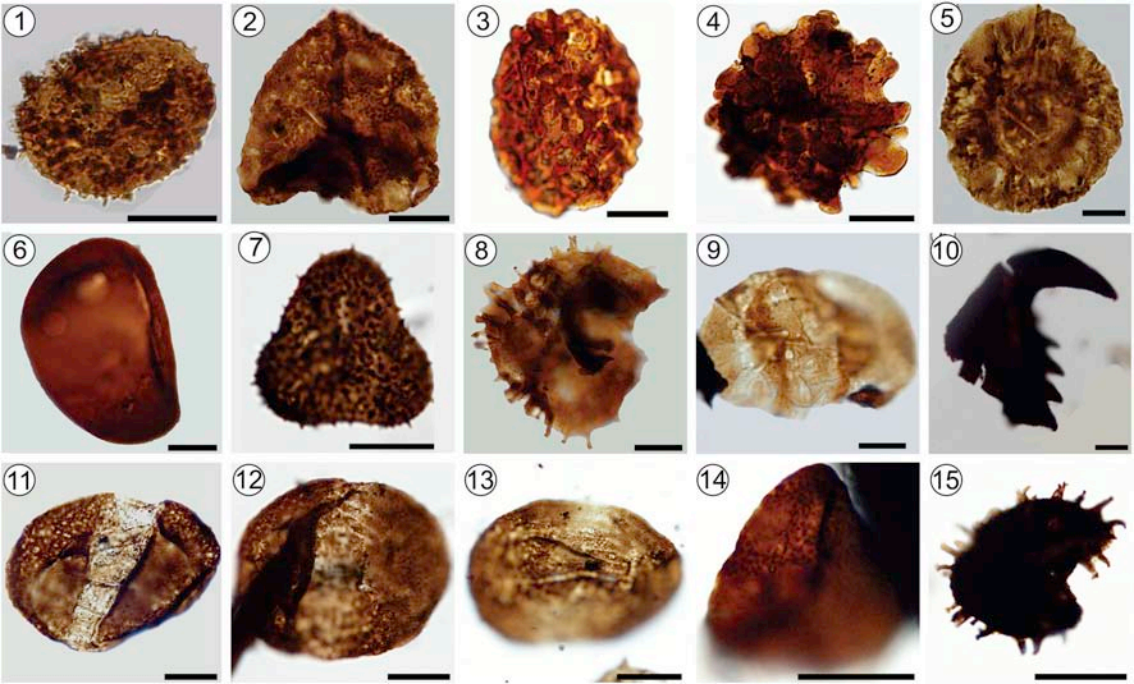
1
2
3
4
5
6
7
8
9
10
11
12
13
14
15

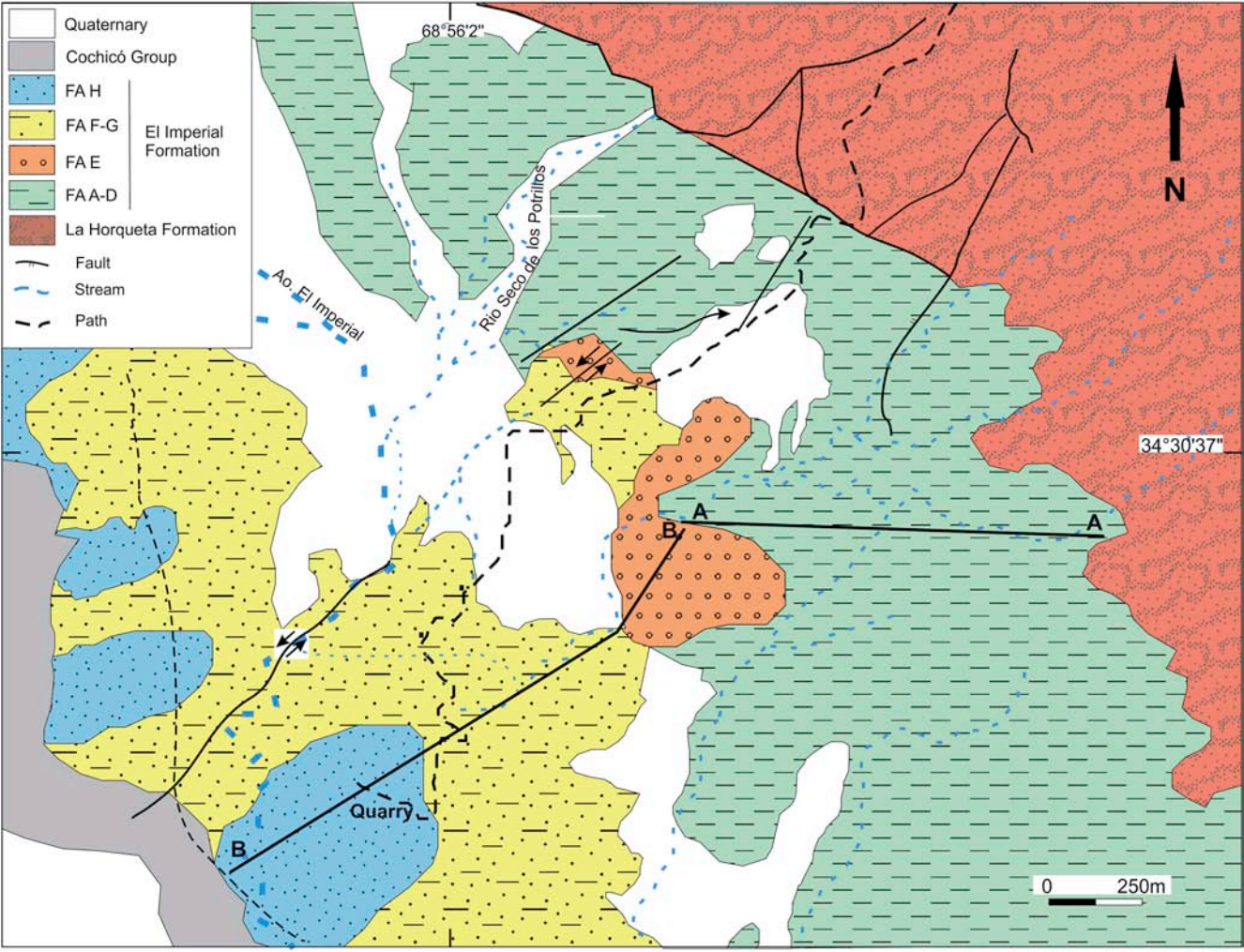
Quaternary
Cochicó Group
FA H
FA F-G
FA E
FA A-D
El Imperial Formation
La Horqueta Formation
Fault
Stream
Path
68°56'2"
34°30'37"
N
Río Seco de los Potrillos
Ao. El Imperial
A
A
B
B
Quarry
0
250m

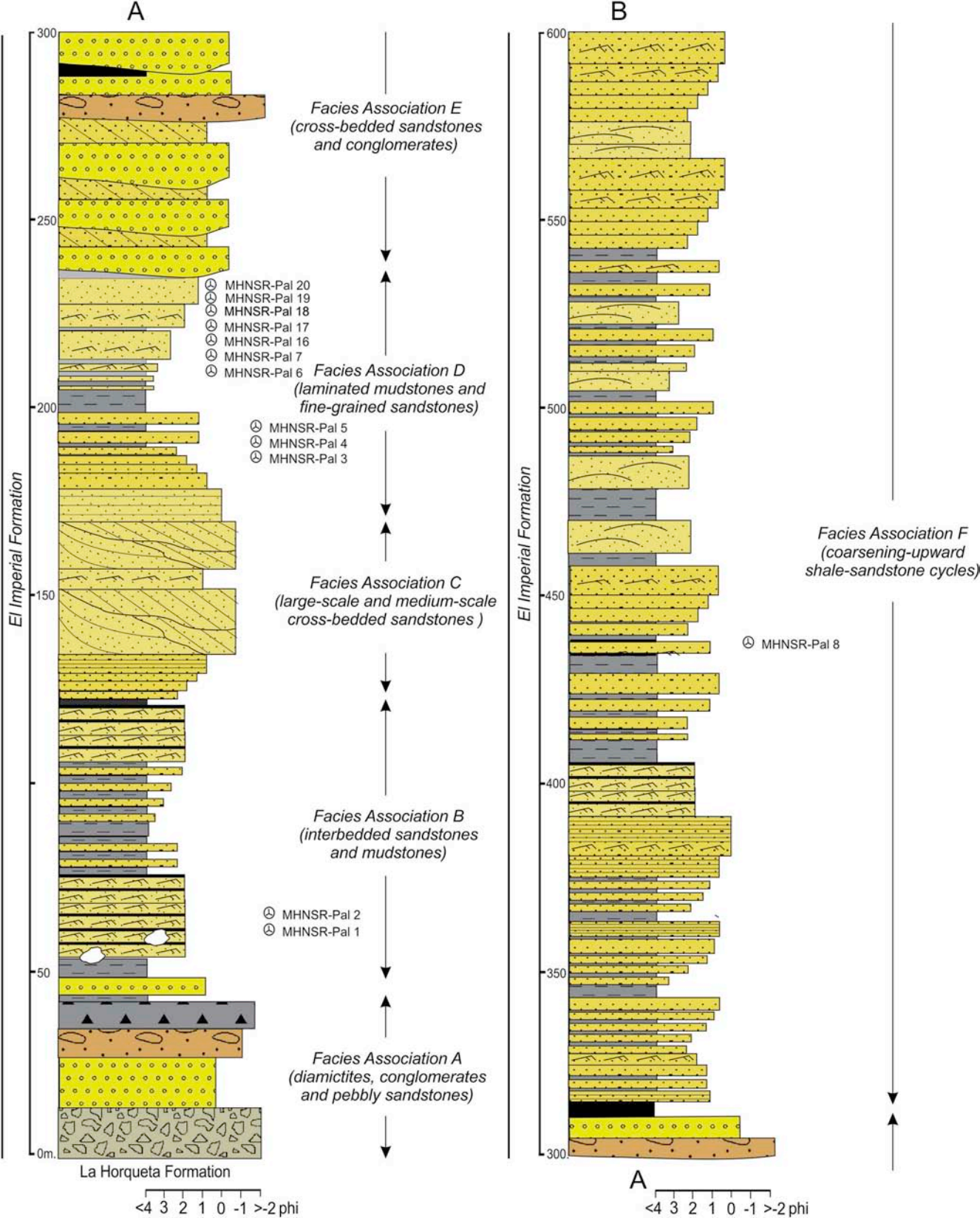
A
B
300
250
200
150
50
0m.
600
550
500
450
400
350
300
El Imperial Formation
El Imperial Formation
Facies Association E
(cross-bedded sandstones
and conglomerates)
Facies Association D
(laminated mudstones and
fine-grained sandstones)
Facies Association C
(large-scale and medium-scale
cross-bedded sandstones)
Facies Association B
(interbedded sandstones
and mudstones)
Facies Association A
(diamictites, conglomerates
and pebbly sandstones)
Facies Association F
(coarsening-upward
shale-sandstone cycles)
MHNSR-Pal 20
MHNSR-Pal 19
MHNSR-Pal 18
MHNSR-Pal 17
MHNSR-Pal 16
MHNSR-Pal 7
MHNSR-Pal 6
MHNSR-Pal 5
MHNSR-Pal 4
MHNSR-Pal 3
MHNSR-Pal 2
MHNSR-Pal 1
MHNSR-Pal 8
La Horqueta Formation
A
<4 3 2 1 0 -1 >-2 phi
<4 3 2 1 0 -1 >-2 phi

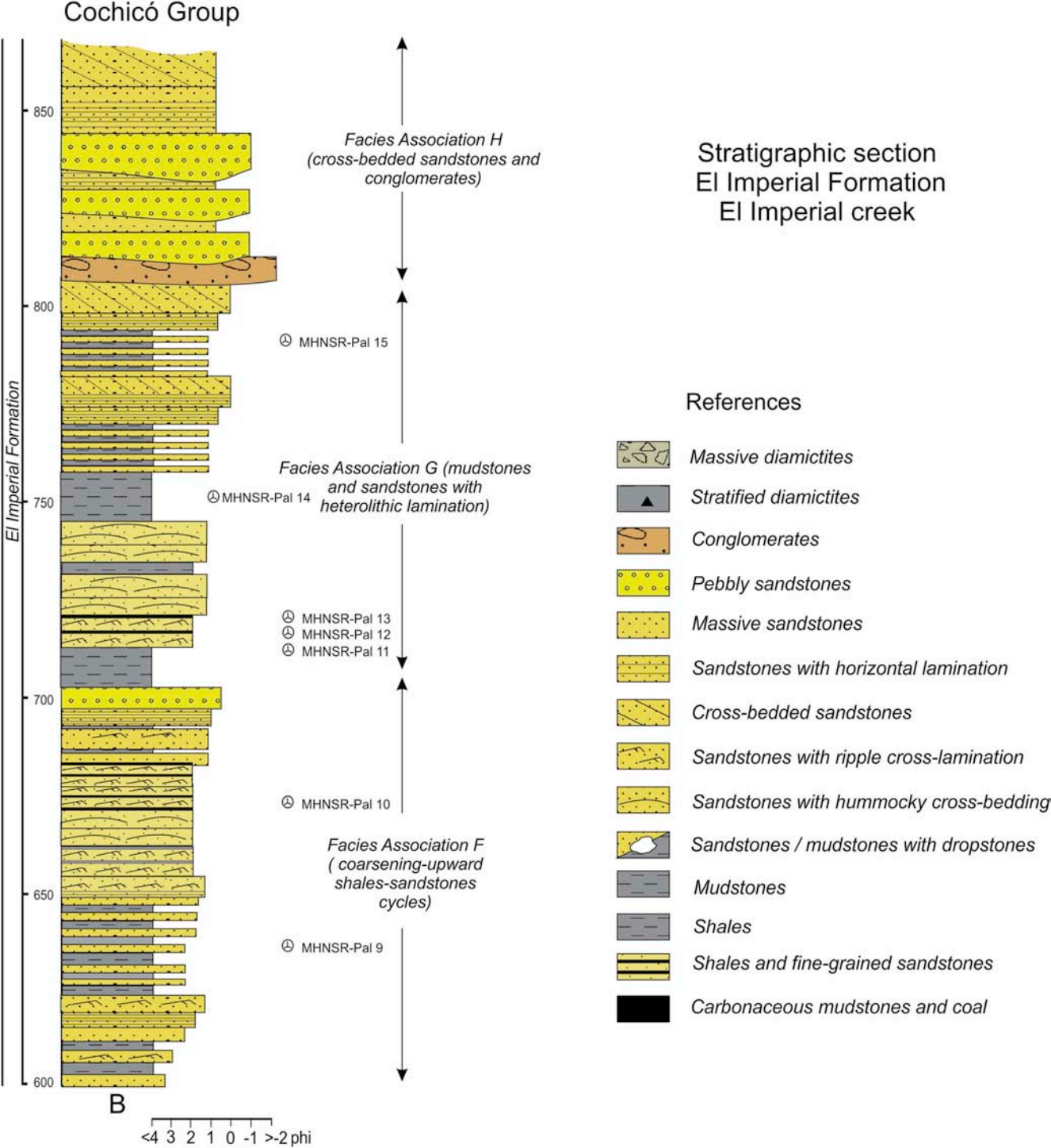
Cochicó Group
El Imperial Formation
850
800
750
700
650
600
Facies Association H
(cross-bedded sandstones and
conglomerates)
MHNSR-Pal 15
Facies Association G (mudstones
and sandstones with
heterolithic lamination)
MHNSR-Pal 14
MHNSR-Pal 13
MHNSR-Pal 12
MHNSR-Pal 11
MHNSR-Pal 10
Facies Association F
(coarsening-upward
shales-sandstones
cycles)
MHNSR-Pal 9
B
<4 3 2 1 0 -1 >-2 phi
Stratigraphic section
El Imperial Formation
El Imperial creek
References
Massive diamictites
Stratified diamictites
Conglomerates
Pebbly sandstones
Massive sandstones
Sandstones with horizontal lamination
Cross-bedded sandstones
Sandstones with ripple cross-lamination
Sandstones with hummocky cross-bedding
Sandstones / mudstones with dropstones
Mudstones
Shales
Shales and fine-grained sandstones
Carbonaceous mudstones and coal

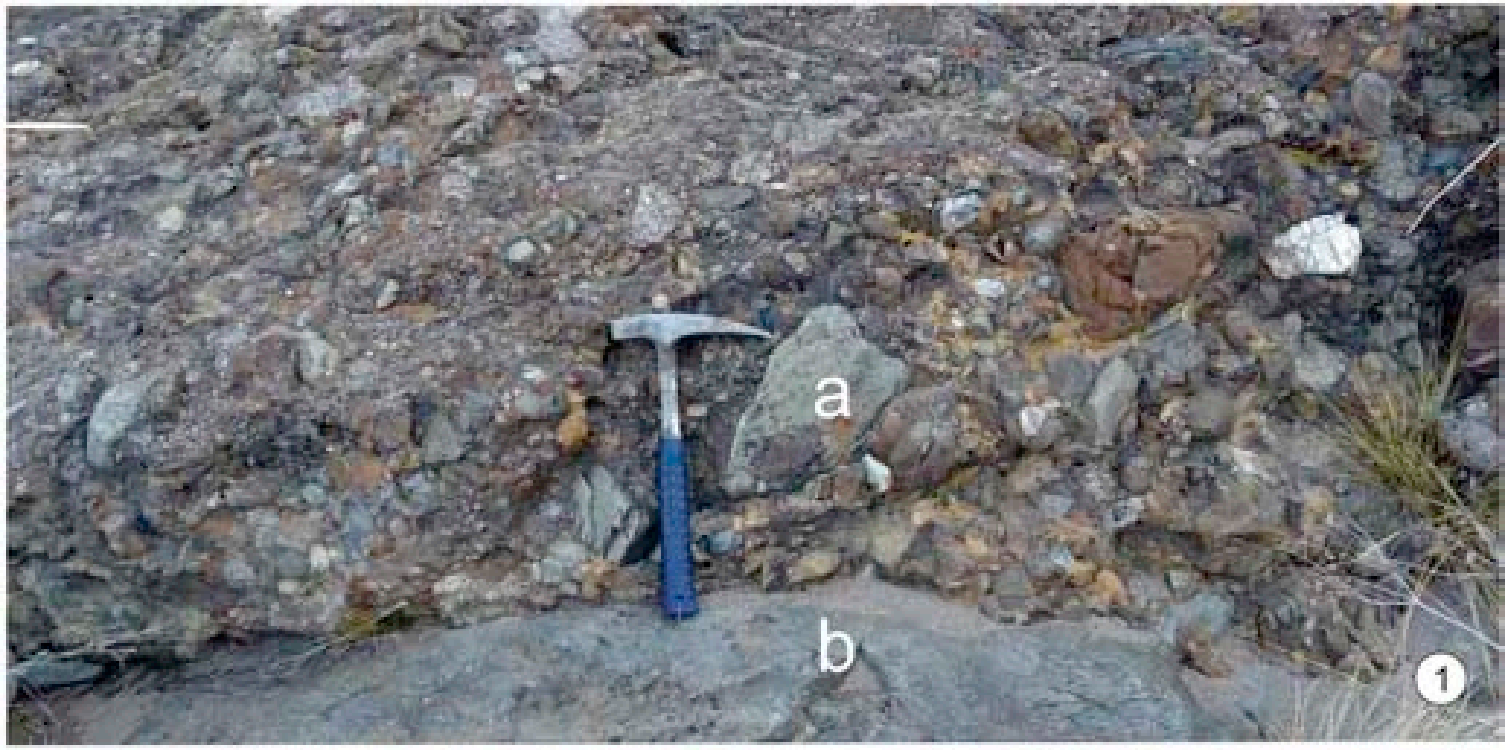
a
b
1

2

3

a
4

1

2

3

4

1

2

3

4

1
2
3
1
2
1
2
1

2

3

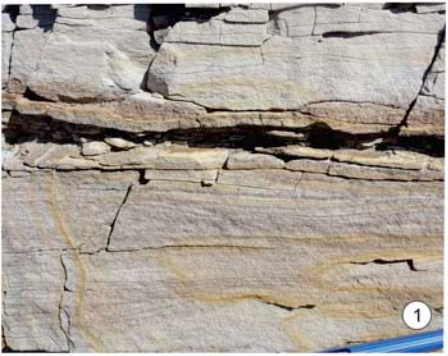
1

2

3

Highlights

. Type section of the El Imperial Formation is revised.
. Eight facies associations represent sedimentation in glacial to postglacial conditions.
. Palynological associations belong to the DM and FS Biozones.
. A continuous late Sepurkhovian-earliest Cisuralian interval is recorded.